The Meteoritical Society

Meteoritics & Planetary Science 46, Nr 10, 1525–1550 (2011)
doi: 10.1111/j.1945-5100.2011.01247.x

Very low strengths of interplanetary meteoroids and small asteroids

Olga POPOVA[1*], Jiří BOROVIČKA[2], William K. HARTMANN[3], Pavel SPURNÝ[2], Edwin GNOS[4], Ivan NEMTCHINOV[1†], and Josep M. TRIGO-RODRÍGUEZ[5]

[1]Institute for Dynamics of Geospheres, Russian Academy of Sciences, Leninsky Prospect 38, Bldg.1, 119334 Moscow, Russia
[2]Astronomical Institute of the Academy of Sciences, Fričova 298, CZ-25165 Ondřejov, Czech Republic
[3]Planetary Science Institute, 1700 E. Ft. Lowell Road, Suite 106, Tucson, Arizona 85719–2395, USA
[4]Muséum d'Histoire Naturelle de Genéve, 1, Route de Malagnou, CP 6434, CH-1211 Genéve 6, Switzerland
[5]Institute of Space Sciences (CSIC-IEEC), Campus UAB, Fac. Ciències, Torre C5-p2, 08193 Bellaterra, Barcelona, Spain
[†]Deceased.
[*]Corresponding author. E-mail: olga@idg.chph.ras.ru

(Received 12 January 2011; revision accepted 26 July 2011)

Abstract–We have assembled data on 13 cases of meteorite falls with accurate tracking data on atmospheric passage. In all cases, we estimate the bulk strength of the object corresponding to its earliest observed or inferred fragmentation in the high atmosphere, and can compare these values with measured strengths of meteorites in the taxonomic class for that fall. In all 13 cases, the strength corresponding to earliest observed or inferred fragmentation is much less than the compressive or tensile strength reported for that class of stony meteorites. Bulk strengths upon atmospheric entry of these bodies are shown to be very low, 0.1 to approximately 1 MPa on first breakup, and maximal strength on breakup as 1–10 MPa corresponding to weak and "crumbly" objects, whereas measured average tensile strength of the similar meteorite classes is about 30 MPa. We find a more random relation between bulk sample strength and sample mass than is suggested by a commonly used empirical power law. We estimate bulk strengths on entry being characteristically of the order of 10^{-1}–10^{-2} times the tensile strengths of recovered samples. We conclude that pre-entry, meter-scale interplanetary meteoroids are typically highly fractured or in some cases rubbly in texture, presumably as a result of their parent bodies' collisional history, and can break up under stresses of a few megapascals. The weakness of some carbonaceous objects may result from very porous primordial accretional structures, more than fractures. These conclusions have implications for future asteroid missions, sample extraction, and asteroid hazard mitigation.

INTRODUCTION: AN EXPANDING CLASS OF METEORITES

Physical properties of small asteroids, e.g., their bulk density, porosity, or mechanical strength, are important quantities both from purely scientific interest (to understand their formation and history) and from possible future practical reasons (mineral mining, impact risk assessment, and mitigation). The mechanical strength is particularly difficult to determine from astronomical observations of asteroids. The strength of meteorites can be measured in a laboratory, but it may not be representative of the bulk strength of the original meteoroid before atmospheric entry and of the asteroid from which the meteoroid was derived. It has been noted in at least some fireball cases in the past that the meteoroids fragmented in the atmosphere under much lower ram pressures than corresponded to the mechanical strength of the recovered meteorites. Ceplecha et al. (1996) specifically noted that the 1992 Peekskill fall fragmented at ram pressure much less than the strength of the similar meteorite classes (0.7–1.0 versus 30 MPa) and suggested that a mechanism other than only ram pressure was probably responsible for this. Other observational data also suggested initial high-altitude fragmentations at exceptionally low ram pressure (Borovička et al. 1998; Petrovic 2001; Brown et al. 2002a; Borovička and Kalenda 2003). In this article,

we undertake a more complete investigation of this phenomenon.

With the rapid proliferation of video recording devices, not to mention the slower expansion of meteor tracking networks, the last few years have marked a dramatic increase in the numbers of meteorite recoveries in which accurate tracking data reveal not only trajectories and orbit information but also details of the multiple fragmentation events as the object passed through the atmosphere. In a certain number of these cases, "ground truth" meteorite samples from the specific fireball have been collected. As Fig. 1 shows, the number of such cases, where both trajectory/fragmentation observations and meteorite samples are available, has increased more or less exponentially in recent years. For the first time, this permits a systematic survey and analytic comparison of a substantial number of these cases, where we can use fragmentation behavior to infer mechanical properties, such as strength, and compare those results with the "ground truth" of the meteorites themselves.

Thirteen cases are known at the time as we completed this article. All 13 cases are stony meteorites. Although the strength of these meteorites was not directly measured in most cases (it is a destructive analysis seldom done), the mineralogical type of the meteorite was determined and we can compare the observed atmospheric fragmentation strength with the laboratory strength of meteorites of the same type. We also complemented our results for the 13 cases by a comparison with data for both smaller and larger meteoroids. Our goal is not only to compare "ground truth" with entry behavior but also to investigate the bulk strength of meteoroids/small asteroids as a function of mineralogical type and the size (or mass) of the body.

DETERMINING THE FRAGMENTATION STRENGTH

It is usually assumed that the destruction of a meteoric body begins at that moment when the aerodynamic pressure in the vicinity of a stagnation point becomes equal to some constant describing the strength of meteoroid material. There are different approaches to the choice of characteristic strength in the breakup criterion (see Svetsov et al. [1995] for some discussion); compressive, tensile, or shear strengths may be utilized by different authors, depending on the assumed mechanism of breakup. We will not consider here the stresses in the meteoroid and mechanism of meteoroid failure. The various kinds of strength measurements are reported by various experiments (cf. Holsapple 2009). As a result of variations in the measurement methodology, these may not be ideal, but

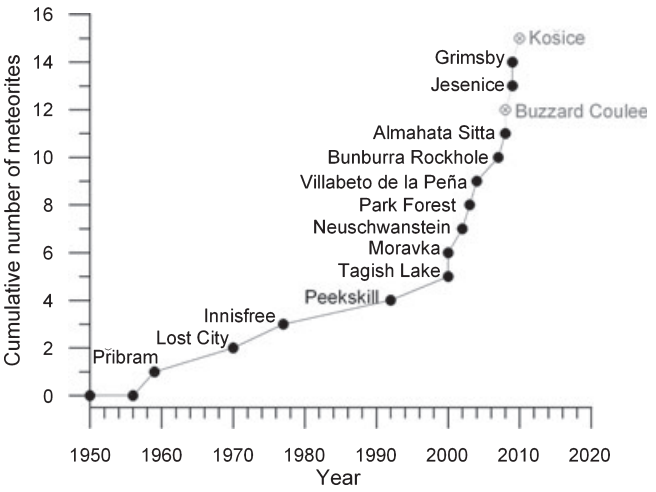

Fig. 1. Cumulative number of detailed observed bolides with recovered meteorites increasing with time. The rate is now about 1–2 per year, and is likely to increase due to growing number of surveillance and amateur video devices in use. Two recent events, whose data are still not available for analysis, are shown by gray symbols (see the Evaluation of Individual Cases section).

we believe that they are adequate to support our conclusion that the strength of the surviving fragments on the ground is systematically larger than the breakup strength of the meteoroid. During the atmospheric loading, the internal stresses in the meteoroid are proportional to the ram pressure (Fadeenko 1967; Tsvetkov and Skripnik 1991), and so we will consider the stagnation pressure at breakup as the breakup criterion and measure of meteoroid strength in the disruption.

We take the fragmentation strength of a meteoroid simply as the loading ram pressure, which caused the fragmentation:

$$p = \rho_h v_h^2, \tag{1}$$

where ρ_h is the atmospheric density at the fragmentation height h, and v_h is the fireball velocity at that height. As the velocity as a function of height is well known from the observations, the issue here is to determine the fragmentation height from fireball data. This can be done by the geometric, dynamic, or photometric methods.

To determine the fragmentation behavior, we need fragment tracking on several subsequent images. The video records showing individual fragments that are available for the Peekskill (Brown et al. 1994; Beech et al. 1995), Morávka (Borovička and Kalenda 2003), and Grimsby (Brown et al. 2011) fireballs, are excellent means to study the fragmentation process in detail. The other possible method is the method of instantaneous exposure (Babadžhanov and Kramer 1968), i.e., long-exposure photographs using rotating shutter with very small open-to-close ratio. On regular long-exposure

photographs, the fragments can be seen only if their trajectories deviate sufficiently from the trajectory of the main body. Such separating fragments have been seen on a number of high resolution fireball photographs, including Příbram, Lost City, and Innisfree (Ceplecha 1961; McCrosky et al. 1971; Halliday et al. 1981). In these cases, the fragmentation heights could be determined easily from geometric intersections of the trajectories.

Another method of revealing fireball fragmentation is based on the fact that the atmospheric deceleration depends on the meteoroid mass. After a sudden mass loss, the deceleration increases. This can be revealed by fitting the fireball dynamics, i.e., the observed length along trajectory as a function of time. The method was elaborated by Ceplecha et al. (1993) and applied to a number of photographic fireballs with sufficiently precise dynamic data. The performance of the method was checked for the Lost City fireball, where the fragmentation points could also be determined geometrically. The method is able to identify the fragmentation events even with only one surviving macroscopic fragment (i.e., when the rest of mass is lost in the form of dust). On the other hand, this method is able to identify only significant mass loss ($>30\%$). The method also has problems in cases of multiple fragmentation events along the trajectory.

The fragmentation events can also manifest themselves on the fireball light curve. The fireball flares, i.e., sudden transient increases of fireball brightness, are caused by the sudden release of large amount of dust or a large number of small fragments. The method, however, cannot reveal the events when only a small number of macroscopic fragments are formed or the amount of dust release is too low. In the radiative radius approach (Nemtchinov et al. 1997; Borovička et al. 1998), the radiative radius is defined from the light curve. This approach is able to determine the position of fragmentation events on the trajectory if the break up occurs at middle and low altitudes. The position of the flares was used to determine the fragmentation heights in the Tagish Lake (Brown et al. 2002a), Park Forest (Brown et al. 2004), Villalbeto de la Peña (Trigo-Rodríguez et al. 2006), Almahata Sitta (Jenniskens et al. 2009), Jesenice (Spurný et al. 2010), and Grimsby (Brown et al. 2011) fireballs.

Recently, the entry of several bolides was reconsidered with the new version of theoretic entry model, so called fragmentation (FM) model by Ceplecha and ReVelle (2005). This model has a large number of free parameters, which need to be estimated at an initial stage and are re-calculated during the solution process. The solution itself is a search of best fit for both to light curve and trajectory data (height as function of time). This model may be used for the cases with high precision observational data, and it reveals positions of fragmentation events and amounts of material lost during each event.

For the sake of completeness, we also note that fireball fragmentation can be studied not only from optical data but also from acoustic/seismic data. The fragmentation events are point sources of sonic waves. The identification of the signatures of individual events in the records of several seismic stations allowed Borovička and Kalenda (2003) to localize fragmentations of the Morávka fireball, which were not covered by the video records. Llorca et al. (2005) also derived the fragmentation height by combining optical, seismic, and infrasound data in the case of Villalbeto de la Peña. Seismic data were crucial for determination of fragmentation height of Jesenice (Spurný et al. 2010). Fragmentation evidences were found on infrasound records of the Grimsby meteorite fall (Brown et al. 2011).

The most difficult fragmentations to detect by any method are the initial breakups of massive meteoroids in the highest parts of their trajectories. The low atmospheric density and relatively large meteoroid mass, even after fragmentation, leads to no measurable deceleration. If only macroscopic fragments are produced, no luminous flare is observed. The geometric separation of massive fragments is also miniscule under the low pressures at high altitudes. That fragmentation occurred becomes evident only below 50 km, when the deceleration becomes much higher than would correspond to the total mass if it were in a single body. In other words, the dynamic mass computed from the deceleration is much lower than the total meteoroid mass determined from other methods. To determine the high-altitude fragmentation, the light data should be analyzed in conjunction with the dynamic data. This has been done for the Benešov (Borovička et al. 1998) and Morávka (Borovička and Kalenda 2003) fireballs. In those cases, we can say that the fragmentation occurred at high altitudes, but we cannot determine the exact fragmentation height. In principle, one cannot exclude the limiting case that the decimeter to m-sized meteoroid itself entered the atmosphere as a swarm of separated bodies, although it is difficult to imagine maintenance of such a swarm over geologic time period prior to Earth encounter.

COMMENTS ON METEOROID MASS ESTIMATES

As we are interested in the meteoroid strength as a function of mass, we must also determine the meteoroid mass from fireball data. The initial mass of the entering meteoroid was estimated using different methods with different accuracy. We collected all mass estimates for the 13 cases under consideration and plot them in Fig. 2.

The dynamic mass is the mass estimate based on the deceleration of the meteoroid along the trajectory. The

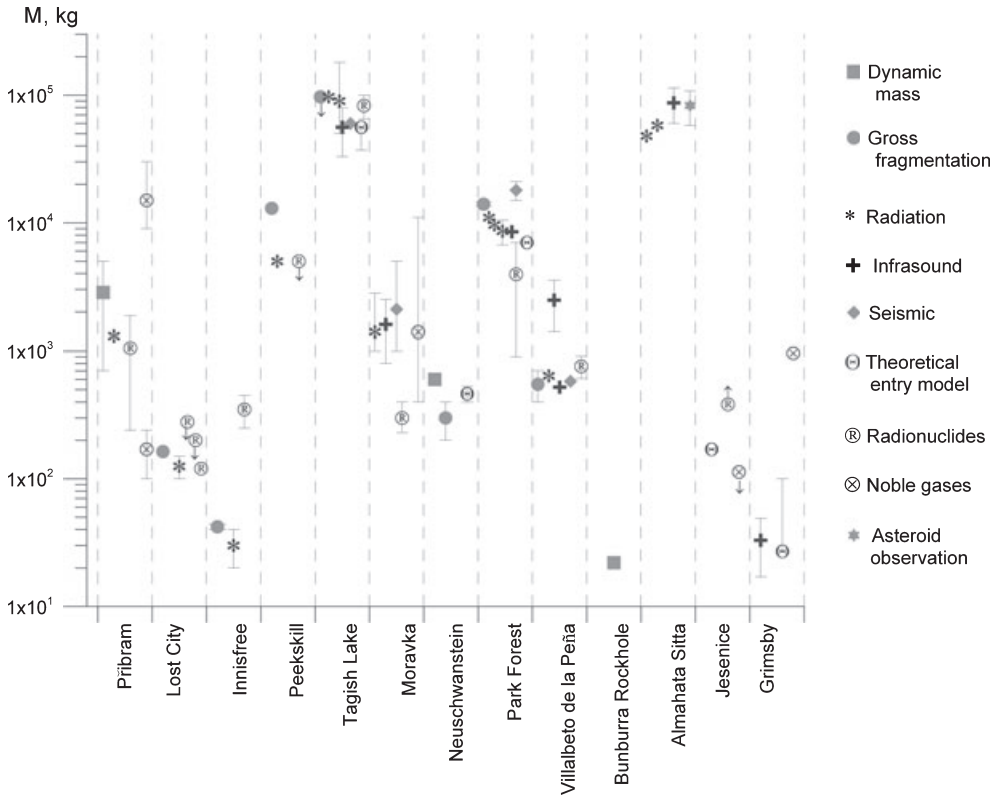

Fig. 2. Comparison of estimates of initial entry mass by different methods, for the fireball/meteorite cases in this paper.

most elaborated method, which estimates the mass based on trajectory data, is the gross-fragmentation approach (Ceplecha et al. 1993; see above). It may be used if the trajectory data are of high quality. Estimates by these methods are identified as "dynamic" and "gross-fragmentation" mass in Fig. 2.

The luminosity method uses groundbased bolide stations' data on the bolide light curve in the panchromatic range (380–640 nm), along with data from visible light satellite-based sensors registering radiation in a wider passband (400–1200 nm; Tagliaferri et al. 1994). Luminous efficiency, i.e., the ratio of irradiated energy to the kinetic energy of the meteoroid, is different in different cases. In general, luminous efficiency varies with meteoroid velocity, size, altitude of flight, and material. Integral luminous efficiency determines the fraction of the bolide initial kinetic energy converted to light in the whole spectrum or in the different passbands. During last 10 years, the estimates of luminous efficiency were fundamentally improved for both observational techniques. Several papers (Ceplecha 1996; Ceplecha et al. 1998; Ceplecha and ReVelle 2005) determine the empirically derived panchromatic luminous efficiency. Theoretic considerations (Golub' et al. 1996) also provide panchromatic luminous efficiency used in modeling (Borovička et al. 1998).

The luminous efficiency for satellite observations was determined theoretically by Nemtchinov et al. (1997). The integral luminous efficiency for satellite observations was also empirically derived using independent energy estimates for those satellite events, which were observed also by other means (Brown et al. 2002b). Mass estimates in Fig. 2 marked "Radiation" use various authors' luminous efficiency values for the various fireball cases.

Meteoroid energy can also be derived from infrasonic and seismic signals. There are several methods of interpretation of infrasonic signal (ReVelle et al. 2004), and so there is usually some mass range derived from infrasound data. Infrasound waves are those below 20 Hz, and attenuation of these waves is very low, so that bolide infrasound can be detected at large distances. Empirical relations have been used between the observed period of the acoustic waves at the maximum amplitude and the source energy, based on large energy, low wave-amplitude nuclear explosion, but there are differences between bolides and nuclear events in terms of energy range and shape of the energy release volume, which add uncertainty in the meteoroid energy and mass estimates (Popova and Nemchinov 2008). In some cases, the difference in energy estimates between the acoustic and latter techniques may be as high as a factor 10 (Brown et al. 2002b).

Different theoretic entry models were also applied to the cases under consideration. These models used various assumptions concerning luminous efficiencies, ablation coefficients, presence of fragmentation, and its treating and material properties. Mass estimates obtained by application of these models we mark as "theoretical entry model" in Fig. 2.

Finally, initial mass of the meteoroid may also be estimated from cosmogenic nuclides production rates and cosmic-ray tracks analyses of the recovered meteorites (marked "Radionuclides" in Fig. 2). The noble gases concentration and isotopic composition also are used and are marked as "Noble gases."

Mass estimates obtained by various methods have a large scatter (Fig. 2). In some cases, masses determined by similar methods for the same meteorite differ in few times and even by the order of magnitude (e.g., the determination of Příbram mass based on the radionuclides).

This scatter is due to the presence of a number of open questions and uncertainties existing in different approaches. If the mass estimates agree with the precision of about two times, we may conclude that these estimates are quite reasonable. A productive area of future work will be the attempt to reconcile the different techniques of energy and mass estimates, and to produce consistent and correct values. We listed the most reliable estimates for the cases under consideration in Table 2.

The relation of the recovered mass to the estimated initial mass is shown in Fig. 3. The recovered masses are typically about 0.1–3% of the initial mass. The found fraction is higher for the two relatively small (initial mass 40 and 160 kg) and slow meteorites in our collection, about 10% of initial mass is recovered for Lost City and Innisfree. The smallest mass fractions are recovered in the case of Tagish Lake and Almahata Sitta meteorites, probably due to their specific composition and structure. The Tagish Lake material has a very high porosity of about 40% (Table 2) (Bland et al. 2004; Consolmagno and Britt 2004; Hildebrand et al. 2006), and its largest fragment constitutes only about 10^{-5} of its initial mass. The Almahata Sitta material porosity is measured as about 15–20% (Kohout et al. 2010, 2011), and asteroid macroporosity is estimated as high as 50% (Welten et al. 2010). The recovered mass is smaller than estimated total fallen mass in all cases, presumably due to inefficiency in finding all fragments.

EVALUATION OF INDIVIDUAL CASES

In this section, we compile the data on 13 well-observed meteorite falls. Although we use the published data, we re-evaluated them critically and supplemented by some quantities not given in the original papers, e.g., the fragmentation heights and ram pressures at

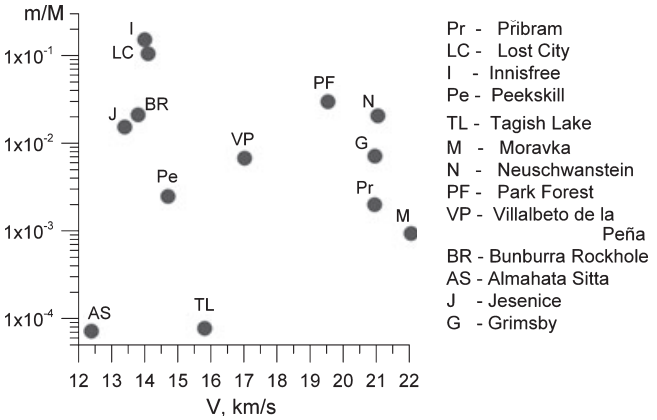

Fig. 3. Ratio of recovered meteorite mass over estimated initial entry mass, plotted against entry velocity.

fragmentations. The comparison of the 13 cases is not trivial, because they were observed by various techniques (even by nonscientific instruments in many cases) showing different kinds of details. Table 1 collects orbital and trajectory data listed in the order of meteorite fall date.

Tables 2 and 3 extends our database with physical properties measured for meteorite samples with additional strength data from similar meteorites. In conjunction with these tables, we next present separate discussions of the 13 individual cases. It should be mentioned here that sufficient data are believed to exist to constrain the orbit for recent Buzzard Coulee H4 ordinary chondrite meteorite (November 21, 2008; Hildebrand et al. 2009) and the Košice H5 chondrite (February 28, 2010; Toth et al. 2010) (Fig. 1). Detailed data are still absent at the time of paper preparation, and so we will not include these events in our tables.

Příbram

Příbram was the first meteorite whose fall was recorded by photographic observations from bolide-recording stations, operated in Czech Republic (Ceplecha 1961).

About 6 kg of material was collected as four stones from the strewn field of about 15 × 1 km. Three meteorites were almost completely covered by fusion crust. Part of the fourth meteorite is free of fusion crust (Ceplecha 1961). These features suggest that fragmentation mostly ceased before ablation ceased (ablation typically stops at the velocity about 2–4 km s^{-1}). Příbram fragments are ordinary chondrites (H5) with a shock stage S1/S3 (Table 2). Its porosity was measured as being zero (Britt and Consolmagno 2003).

The dynamic mass of Příbram was estimated as about 700–5000 kg (Ceplecha 1961). Parent mass estimates from noble gases and unstable isotope data by

Table 1. Orbital and trajectory data for 13 bolides with recovered meteorites (epoch of the elements for individual bolides is J2000.0 except Lost City and Innisfree [1950.0]).

Bolide event	Fall date	Orbit a	Orbit q	Orbit Q	Orbit e	Orbit i	Entry velocity (km s^{-1})	Trajectory slope (°)	H_B (km)	H_E (km)	I_{max} (mag)
Příbram[a,b]	4/7/1959	2.401	0.78951	4.012	0.6711	10.482	20.9	43	98	13	−19
Lost City[c,g,j]	1/4/1970	1.66	0.97	2.35	0.417	12	14.1	38	86	19	−12
Innisfree[d,e]	2/6/1977	1.872	0.986	2.758	0.47	12.27	14.5	68	> 62	20	−12
Peekskill[f,g]	10/9/1992	1.49	0.886	2.1	0.41	4.9	14.7	3	60	34 (30)	−16
Tagish Lake[h]	1/18/2000	2.1	0.89	3.3	0.57	1.4	15.8	16.5	–	29	−22
Morávka[i,j]	5/6/2000	1.85	0.98	2.71	0.47	32.2	22.5	20	80	21	−20
Neuschwanstein[b]	4/6/2002	2.40	0.7929	4.01	0.670	11.41	20.95	49	85	16	−17.2
Park Forest[k]	3/27/2003	2.53	0.811	4.26	0.68	3.2	19.5	61	82	18	−21.7
Villalbeto de la Peña[l]	1/4/2004	2.3	0.86	3.7	0.63	0.0	16.9	29	–	22	−18
Bunburra Rockhole[m,n]	7/20/2007	0.8514	0.6428	1.05996	0.245	9.07	13.4	30.9	62.8	29.6	−9.3
Almahata Sitta[o,p]	10/7/2008	1.308	0.8999	1.7164	0.3121	2.54	12.42	20	65?	32	−19.7
Jesenice[q]	4/9/2009	1.75	0.9965	2.51	0.43	9.6	13.8	59	88	(18)	−15
Grimsby[r]	9/26/2009	2.04	0.9817	3.09	0.518	28.07	20.91	55.2	100	19.6	−14.8

Source: [a]Ceplecha (1961); [b]Spurný et al. (2002, 2003); [c]McCrosky et al. (1971); [d,e] Halliday et al. (1978, 1981); [f]Brown et al. (1994); [g]Ceplecha et al. (1996); [h]Brown et al. (2000, 2002a); [i]Borovička et al. (2003a); [j]Borovička and Kalenda (2003); [k]Brown et al. (2004); [l]Trigo-Rodríguez et al. (2006); [m]Spurný et al. (2009); [n]Bland et al. (2009); [o]Jenniskens et al. (2009); [p]Borovička and Charvat (2009); [q]Spurný et al. (2010); [r]Brown et al. (2011).

Table 2. Physical data for meteorites from 13 bolides with well-measured trajectories.

Bolide event	Inferred initial mass (kg)	Inferred initial diameter (cm)	Type	Shock grade (S)	Density (g cm^{-3})	Porosity (%)	Exposure age (Ma)
Příbram	1300[a]	90	H5[w]	1/3	3.57[o]	0[o]	29–36[t]; 18–26[u]; 12[x]
Lost City	160[b,k]	45	H5[w]	4	3.4 ± 0.18[uu,o,p]	6.0 ± 4.5[uu,p]	5.5[y]; 8–10[z]
Innisfree	40[c,k]	28	L5[w]	2	3.35 ± 0.16[uu,o,p]	5.8 ± 4.7[uu,p]	26–28[yy]
Peekskill	5000[a]	140	H6[w]	2	3.4 ± 0.18[uu,o,p]	6.0 ± 4.5[uu,p]	32[zz]
Tagish Lake	65,000[d]	420	C2, C[m,n]	1[m,n]	1.64[v]	40 ± 1[v]	> 5.5[xx]
Morávka	1500[a]	93	H5-6[l]	2[l]	3.59[l]	< 1[l]	6.7[l]
Neuschwanstein	300[e]	55	EL6[e,s]	2[s]	3.492[q]	(9.3 ± 3.9, model)[uu,p]	48[e]
Park Forest	10,000[f,j]	180	L5[f]	5[f]	3.35 ± 0.16[uu,p]	5.8 ± 4.7[uu,p]	?
Villalbeto de la Peña	600[i]	70	L6[g]	4[g]	3.42 ± 0.10[g]	4.7 ± 0.1[g]	48 ± 5[g]
Bunburra Rockhole	22[nn]	24	Achondrite-anomalous[nn,w]	Minimal[w]	2.86 ± 0.07[uu,o,p]	7.8 ± 6.8[uu,o,p]	–
Almahata Sitta	70,000[i]	400[jj]	Ureilite-an[jj]	–	2.3 ± 0.2[jj] 2.5 ± 3.1[mm]	15–20[mm]	–
Jesenice	170[qq]	45[qq]	L6[qq]	3[tt]			~3.5[kk]
Grimsby	30[rr]	13[rr]	H4-6[rr]		3.37 ± 0.3[pp]	6.7 ± 0.8[pp]	~21.4–26[ss]

Source: [a]Borovička and Kalenda (2003); [b]Ceplecha (1996); [c]Halliday et al. (1978); [d]Brown et al. (2002a); [e]Spurný et al. (2003); [f]Simon et al. (2004); [g]Llorca et al. (2005); [i]This paper; [j]Brown et al. (2004); [k]Ceplecha and ReVelle (2005); [l]Borovička et al. (2003b); [m]Zolensky et al. (2002); [n]Consolmagno and Britt (2004); [o]Britt and Consolmagno (2003); [p]Britt and consolmagno (2004); [q]Kohout et al. (2004); [s]Bischoff and Zipfel (2003); [t]Fireman and DeFelice (1964); [u]Lavrukhina et al. (1974); [v]Hildebrand et al. (2006); [w]Meteoritical Bulletin Database (http://tim.er.usgs.gov/meteor/metbull.php); [x]Stauffer and Urey (1962); [y]Bogard et al. (1971); [z]Englert (1985); [xx]Nakamura et al. (2003); [yy]Goswami et al. (1978); [zz]Graf et al. (1997); [nn]Bland et al. (2009); [mm]Kohout et al. (2010, 2011); [jj]Jenniskens et al. (2009); [qq]Spurný et al. (2010); [rr]Brown et al. (2011); [kk]Ott et al. (2010); [pp]McCausland et al. (2010); [ss]Cartwright et al. (2010); [tt] Bischoff et al. (2010b).

[uu]Not measured directly for the given meteorite but taken as an average for the given class.

Table 3. Physical data for meteorites from 13 bolides with well-measured trajectories.

				Measured strength of similar meteorites		First breakup		Maximum strength at breakup	
Bolide event	Weight expected (kg)	Weight recovered (kg)	Fragments number	Compressive (MPa)	Tensile (MPa)	Inferred bulk strength (MPa)	Altitude (km)	Inferred bulk strength (MPa)	Altitude (km)
Příbram	80[a]	6[a]	4[a]	77–247	31–42	0.9	44	–	–
Lost City	25[b]	17[b]	4[b]	77–247	31–42	0.7	41	2.8	28
Innisfree	5[c]	4.6[c]	9[c]	20–450	(2–62)	0.1	55.6	3	23.7
Peekskill	?	12.4[l]	1[l]	163–327	–	–	41.6		36
Tagish Lake	100–1000[d]	16.3[d]	~500[d]	–	–	0.3	48	2.2	32
Morávka	100[a]	1.4[a]	6[a]	77–327	31–42	< 0.9	> 46	5	29.3
Neuschwanstein	20[e]	6.2[k]	3[k]	–	–	3.6	34	9.6	20.8
Park Forest	> 45[f,g]	30[f,g]	> 100[f,g]	20–450	2–62	0.03	70	7	29
Villalbeto de la Peña	?	4.4[h,j]	33[h,j]	63–98	6–31	–	–	5.1	24
Bunburra Rockhole	1.1[n,m]	0.339[n,i]	3[n,m,i]	–	–	0.1	54.8	0.9	33.9
Almahata Sitta	?	~5[o]	> 300[o]			0.2–0.3	46–42	1	33
Jesenice	10–30[p]	3.6[p]	3[p]	63–98	6–31	0.3	46	3.9	23
Grimsby	5[q]	0.215[q]	13[q]	77–327	31–42	0.03	70	3.6	30

Source: [a]Borovička and Kalenda (2003); [b]Ceplecha (1996); [c]Halliday et al. (1978); [d]Hildebrand et al. (2006); [e]Spurný et al. (2002, 2003); [f]Simon et al. (2004); [g]Brown et al. (2004); [h]Llorca et al. (2005); [i]This paper; [j]Trigo-Rodríguez et al. (2006); [k]Oberst et al. (2004); [l]Brown et al. (1994); [m]Bland et al. (2009); [n]Spurný et al. (2009); [o]Jenniskens et al. (2009); [p]Spurný et al. (2010); [q]Brown et al. (2011).

different authors have a large scatter from 240–1900 kg (Bagolia et al. 1980) to 15,000 kg (Lavrukhina et al. 1974). The light curve of Příbram was partially overexposed, and so its photometric mass was only estimated. Its initial mass was reconsidered recently as about 1300 kg (Borovička and Kalenda 2003).

The continuous separation of individual fragments from the main trajectory was visible, beginning at an altitude of about 44 km. The points of separation of 17 individual fragments were found by direct intersections of the fragments trajectories with the main one. The fragments were formed at 44–23 km altitudes, and the apparent strength may be estimated as 0.9 MPa at first breakup, then increasing probably up to approximately 10–14 MPa taking into account atmospheric density increase. The velocity was measured at an altitude of > 40 km only (Ceplecha 1961) and the strength values at low altitudes may be overestimated.

Lost City

The Lost City meteorite was photographed in flight and recovered by the Prairie Network (USA) in 1970 (McCrosky et al. 1971). Lost City had a low entry velocity, a relatively high amount (~10%) of its initial mass (~160 kg; Tables 2 and 3) survived the atmospheric passage and was collected on the scattering field of about 1.2 × 1.2 km. Four fragments totaling 17 kg have been found, the largest fragment having mass approximately 9.83 kg (McCrosky et al. 1971). Lost City is an ordinary chondrite (H5) in S4 shock stage. All recovered meteorite fragments are completely covered by fusion crust, again indicating that fragmentation mostly ceased before ablation ceased.

Modeling of the Lost City entry confirmed several stages of disruption of the meteoroid during its flight and the importance to take the fragmentation events into account in modeling (Ceplecha 1996; Nemtchinov et al. 1997).

The initial mass of Lost City according the FM model (Ceplecha and ReVelle 2005) was about 163 ± 5 kg. They also found 10 fragmentation points, six of them above 40 km. The model also provides the mass of the main body before and after each fragmentation. Most fragmentation events are small, the estimated mass losses are smaller than 2.3%, and all mass is released in the form of dust. Their best solution includes four main fragmentation points (at 41, 38, 28, and 22 km altitudes). Three of them (at 41, 28, and 22 km) were previously found geometrically by trail intersections and two (at 28 and 22 km) were also found by radiative radius modeling (Nemtchinov et al. 1997). The amounts of mass lost during these fragmentation events are 59.5%, 16%, 20%, and 50% of the mass before the fragmentation. The main mass separated in the form of large fragments. The apparent strength was 0.7, 0.95, 2.8, and 1.7 MPa if the deceleration curve from Ceplecha and ReVelle (2005) is used.

Innisfree

The Innisfree meteorite was the third fall for which accurate orbital data were recorded by a camera Network (MORP, Canada; Halliday et al. 1978, 1981). Nine meteorite fragments totaling 4.58 kg mass were collected in a small scattering field of about 0.5 × 1 km, the largest stone being 2.07 kg. The initial mass of the Innisfree meteoroid is estimated to be as low as 20–40 kg (Halliday et al. 1981) and the recovered fragments constitute approximately 15% of the original mass (Tables 2 and 3). The meteorites were classified as type L5, S2 (Rubin 1994).

The individual pieces were covered with the usual thin black fusion crust. One face of the main piece shows an area of partial fusion crust, where a thin layer may have broken off when the velocity was too low to generate a fresh crust.

The lower part of the photographic trail recorded at one of the stations shows the flight of six fragments. The altitudes of fragment appearance are in the range about 24.7–30.3 km. The inferred separation heights from the main body are 25–55 km.

Ceplecha and ReVelle (2005) applied their FM model to the Innisfree bolide. They estimated the initial mass of the Innisfree meteoroid at 42 kg, slightly larger than the previous estimate (see above). They found nine fragmentation events, mass losses in four of them exceeding 20%. The main breakups are found at altitudes of 55.6, 46.2, 36, and 23.72 km, corresponding to relative mass losses of 30%, 42%, 20%, and 61%. The apparent strengths at these fragmentation events are 0.1, 0.3, 1.3, and 3 MPa taking into account the deceleration curve given by Ceplecha and ReVelle (2005).

Peekskill

Peekskill, a 1992 fall, was the fourth recovered meteorite for which detailed and precise data on the meteoroid atmospheric trajectory and the orbit exist. A bright fireball lasting more than 40 s was recorded by 15 chance eyewitnesses' videocameras from different locations.

A meteorite with a mass 12.4 kg struck a parked car at Peekskill, New York (USA). This meteorite is classified as H6, S2. It is nearly completely covered by a fusion crust (Brown et al. 1994).

Data analysis shows that Peekskill was an Earth-grazing event, the third such case known (Ceplecha et al. 1996). Two high resolution photographs show extreme fragmentation of the body. Extensive fragmentation starts at an altitude of about 41.5 km (Brown et al. 1994; Beech et al. 1995). At least 70 pieces of different size were seen by the time the object reached the height of 38.6 km, their longitudinal displacement along the trajectory reaching about 20 km, and transverse displacement for some small fragments reaching about 1 km. A significant flare attributed to fragmentation was recorded at an altitude 36.2 km.

The apparent bulk strengths at the points of fragmentations are estimated as 0.7–1 MPa (Ceplecha et al. 1996). The initial mass of Peekskill was estimated at 10,000 kg by fireball dynamic data and < 5000 kg from radionuclide data. Borovička and Kalenda (2003) re-estimated the initial Peekskill mass as 5000 kg taking into account the brightness estimate and comparisons with other bolides.

Making a compilation of Peekskill data available in several papers (Brown et al. 1994; Beech et al. 1995; Ceplecha et al. 1996), we adopted three point of essential fragmentation (at about 41.6, 36, and 31 km altitudes). In these cases, the strength at the breakups would be about 0.7, 1, and 0.5 MPa. We should note here that the estimates for Peekskill are crude, due to the quality of data extracted from observation, which still are waiting for the detailed analysis. We also cannot exclude the possibility of an earlier fragmentation. The values of masses at fragmentation points are also very uncertain.

Tagish Lake

Tagish Lake is the only carbonaceous chondrite in our list of bolides and falls. It is classified as ungrouped C2 chondrite with composition intermediate between CM and CI meteorites (Brown et al. 2000). The fireball producing the Tagish Lake meteorite occurred on January 18, 2000, in Canada and was registered by the satellite network, by local seismic stations and infrasound recording, and by scattered videorecordings of the dust trail left in the atmosphere (Brown et al. 2002a).

More than 500 meteorites were recovered from a strewn field approximately 16 × 3 km. The largest meteorite has a mass of about 2.3 kg, and the smallest ones are less than a gram in mass (Brown et al. 2000).

Estimates of initial mass vary widely from 33,000 to 200,000 kg (Brown et al. 2001, 2002a). The best initial mass estimate is about 65,000 kg (Brown et al. 2001) or 56,000 kg (Brown et al. 2002a). A later paper by Hildebrand et al. (2006) suggests mass estimate as 60,000–90,000 kg, based on cosmogenic nuclide study.

According to Brown et al. (2002a), the height of the earliest fragmentation is 48 km, the height of the initial major fragmentation is 37 km. This gives the apparent strength of 0.3 and 1.3 MPa, respectively. We re-estimate loading pressure values given by Brown et al. (2002a) based on their deceleration curve and altitudes of breakup. The crushing strength appears to be in the same range as for meteoroids with ordinary chondritic composition (see Table 3), despite the essential difference in composition.

Morávka

The Morávka fireball appeared over Poland and the Czech Republic on May 6, 2000, during daytime. Three video records of the fireball were obtained by scattered witnesses, together with rich seismic and infrasonic data. The fireball trajectory and orbit were determined by Borovička et al. (2003a). The initial mass of the meteoroid was 1500 ± 500 kg (Borovička et al. 2003b). Six ordinary chondrites of the type H5-6 with total mass of 1.4 kg have been recovered up to now, although it was estimated that the total mass fallen is of the order of 100 kg (Borovička and Kalenda 2003). None of the recovered meteorites was fully covered by the fusion crust. The meteorite bulk density is 3.59 g cm^{-3}, the shock stage is S2, and the porosity was estimated to be about 1% only (Borovička et al. 2003b).

Despite the overall compactness of the recovered meteorites, the fireball experienced extensive fragmentation during the atmospheric flight (Borovička and Kalenda 2003). There is dynamic evidence of high-altitude fragmentation under ram pressures < 0.9 MPa. The primary fragments, of approximately 100 kg, then experienced other break-ups at the heights 36–29 km under ram pressures approaching 5 MPa. Interestingly, the cascade fragmentation continued at lower heights when the fragments have been decelerated and the ram pressure decreased down to 2 MPa. The video record shows about a hundred fragments in flight. Borovička and Kalenda (2003) studied the fragmentation sequence in detail and found that a significant part of the mass was lost in the form of dust or tiny particles, which seems to be the dominant mechanism of the meteoroid mass loss.

Neuschwanstein

The Neuschwanstein meteorites fell in southern Germany on April 6, 2002. The event was captured by seven all-sky cameras of the European Fireball Network (EN), by two radiometers, two infrasound arrays, and nine seismic stations (Spurný et al. 2002, 2003; ReVelle et al. 2004). The initial mass was determined from the dynamics with the most probable value of 300 ± 100 kg. About 7% of the initial mass is expected to have reached the ground. After extensive search in difficult high-mountain terrain, three fragments of total mass of 6.22 kg were found in the predicted impact area. They are classified as a rare EL6 enstatite chondrite. The meteorite density is 3.492 g cm^{-3} (Kohout et al. 2004) and the shock stage is S2 (Bischoff and Zipfel 2003). All meteorite fragments have a complete fusion crust (Oberst et al. 2004), suggesting no further fragmentation after the ablation phase.

There is no direct evidence of fragmentation from the photographic records, because the resolution of the images did not allow distinguishing individual fragments. Similarly, the dynamics information is not sufficiently accurate to describe the fragmentation history of the event. However, from the radiometric record, the light curve was constructed (Spurný et al. 2002) and at least three significant flares are well distinguishable. This probably implies fragmentation processes at these points. As can be seen from Table 4, these flares correspond to the heights of 34, 30, and 20.8 km with the most severe fragmentation at the terminal flare at an altitude of 20.8 km. The corresponding ram pressures are 3.6, 6.0, and 9.6 MPa. The last breakup at the altitude of 20.8 km under ram pressure of 9.6 MPa is the highest value from all 13 studied cases, and this value is one of two exceptionally high values among all known fireballs with known fragmentation history (see the Summary of 13 Meteorite Falls section), although the values for Příbram may have been similar.

Two meteorites in our list of 13, Příbram and Neuschwanstein, have nearly identical orbital elements (Table 1). However, the taxonomic classes and cosmic-ray exposure (CRE) ages are different (Table 2). Pauls and Gladman (2005) calculated the ''decoherence time'' for imaginary streams of meteoroids spread along the same orbit to arrive in dissimilar orbits under perturbation models including all nine planets. They found that a ''Příbram stream'' would decohere in only about 50,000 years, only 1–2% of the CRE ages of these objects. They concluded that there is no genetic relation between Příbram and Neuschwanstein.

Park Forest

In 2003, a large meteorite broke up and fell upon the south suburbs of Chicago (USA). Hundreds of fragments have been recovered, with a total mass of approximately 30 kg. The largest stone is 5.26 kg (Brown et al. 2004; Simon et al. 2004). The fall was recorded by groundbased videos, satellite system, infrasound, and seismic and acoustic instruments. The meteorites were classified as strongly shocked (S5) L5 chondrite. Recovered specimens range from nearly fusion crust-free to completely crusted (Simon et al. 2004).

Three main fragmentation events were identified, at altitudes of 37, 29, and 22 km, based on video and satellite data (Brown et al. 2004). Seismic and acoustic recordings show evidence of fragmentation at 42, 36, 29, and 17 km. Brown et al. (2004) found also clear hints of an early, minor fragmentation in the video record near 70 km altitude under small ram pressure of 0.03 MPa. The fragmentation at 37 km is estimated to occur at the loading of about 2.4 MPa, the major burst at 29 km—under loading of about 7 MPa.

The initial mass was estimated with different methods and the total range of predictions is wide—from

Table 4. Atmospheric fragmentation data for meteorites.

		Fragmentation point			Mass (kg)		
Bolide event	Method	Height (km)	Velocity (km s^{-1})	Ram pressure (MPa)	Before	After	References
Příbram	G	44	20	0.9	1200		Ceplecha (1961)
	G	40.5					
	G	32.2					
	G	27.9					
	G	23.3					
Lost City	M, G, D	41	14	0.7	153	62	Ceplecha and ReVelle (2005)
	M, G	38	13.4	0.95	60	50	
	M, G	28	10.5	2.8	38	30	
	M, G, D	22	5.2	1.7	22	11	
Innisfree	M, G	55.6	14.5	0.1	39	27	Ceplecha and ReVelle (2005)
	M	46.2	14.5	0.3	26	15	
	M, G	36	13.5	1.3	14	11	
	M, G	23.7	7.8	3.0	7	3	
Peekskill	D, G	41.6	13.7	0.7	3000	(300)	Ceplecha et al. (1996);
	F	36	12	1	(200)	(80)	Beech et al. (1995);
	D, G	30.5	5.4	0.5	(40)	(12)	Brown et al. (1994)
Tagish Lake	F	48	15.5	0.3	52,000	50,000	Brown et al. (2002a)
	F	37	15	1.3	48,000	1000?	
	F	32	13	2.2	500?	10?	
Morávka	D	> 46	22	< 0.9	1500	200	Borovička and Kalenda (2003)
	D	29.3	15.9	5.0	77	47	
	D	24.0	7.2	2.3	12	7	
Neuschwanstein	F	34	19	3.6	300		Spurný et al. (2002, 2003)
	F	30	18	6.0			
	F	20.8	12	9.6	100		
Park Forest	D	70	19.5	0.03	10,000		Brown et al. (2004)
	D	37	19.5	2.4			
	D	29	18	7			
	F	22	10?	6.5?			
Villalbeto de la Peña	F	30	14.8	3.9	530	500	Trigo-Rodríguez et al. (2006)
	F	28	14.2	4.8	450	130	
	F	24	10.5	5.1	37	14	
Bunburra Rockhole	D, F, M	54.9	13.2	0.11	21.5	8.6	Spurný et al. (2009, 2011);
	D, F, M	37.8	11.3	0.74	5.5	3.96	Bland et al. (2009)
	D, F, M	37.3	11.0	0.77	3.9	3.5	
	D, F, M	35.85	10.4	0.85	3.5	1.9	
	D, F, M	33.6	9.1	0.9	1.7	1.53	
	D, F, M	31.3	7.6	0.89	1.4	1.26	
Almahata Sitta	F, C	45	12.3	0.3	70,000	(50,000)	Jenniskens et al. (2009);
	F, C	37	11.9?	0.9	(45,000)	(5000)	Borovička and Charvat (2009)
	F	33	10.9?	1.3	(3000)		
Jesenice	S, M	46	13.6	0.3	170	40	Spurný et al. (2010)
	F, S, M	26	10.9	3.6	35	4	
	F, S, M	25	10	3.6	22	5	
	F, M	23	8.6	3.9	21	5	
	F, M	19	6	3.2	20	1	
Grimsby	Rd, I	70	20.9	0.03	30		Brown et al. (2011)
	F, M, I	50	20.5	0.1			
	F, G, M	39	19.5	1.5			
	F, G, M	33	17	3.2			
	F, G, M	30	13	3.6			

Note: D = dynamics; F = flare; G = geometry; M = modeling; C = dust cloud; S = seismic location; Rd = radar data; I = infrasound.

as low as 900–7000 kg based on radionuclide data (Simon et al. 2004), up to 14,000–18,000 kg based on gross-fragmentation model and seismic data (Brown et al. 2004). The most probable initial mass estimate is about 10,000 kg.

Villalbeto de la Peña

The Villalbeto de la Peña fireball appeared over Spain on January 4, 2004, during daytime. Thirty-three L6 ordinary chondrites (S4) with total mass of about 5 kg have been recovered so far, most of them being covered by fusion crust (Llorca et al. 2005; Trigo-Rodríguez et al. 2006). The size of the strewn field is about 20 × 6 km (Llorca et al. 2005).

One video record and two photographs of the fireball in flight were obtained by scattered witnesses. Numerous photographs of the dust train left by the fireball were also taken. Seismic and infrasonic data are available as well. The fireball trajectory and orbit was determined by Trigo-Rodríguez et al. (2006). The initial mass of the meteoroid was found to be 760 ± 150 kg by combining luminosity, seismic, infrasound, and cosmogenic radionuclides data (Llorca et al. 2005). The modeling of dynamics and light curve from the video record by Trigo-Rodríguez et al. (2006) gave the mass at the beginning of the video record ($h \sim 33$ km) of 550 ± 150 kg, corresponding to the initial mass of about 600 kg.

One of the fireball photos and a few video frames show fragments separated from the main body, but the data are insufficient to track the individual fragments. The fireball light curve extracted from the video shows at least seven flares, the most pronounced one occurring at the height of 28 km. The first flare was observed at the height of 30 km under the ram pressure of 3.9 MPa, but no one can exclude the earlier fragmentation, and so we do not enter a strength value for the first breakup into Table 3. The ram pressure at the main flare was 4.8 and 5 MPa at the position of the last flare at 22 km. The amplitude of the flares and the existence and appearance of the dust train shows that most mass loss in fragmentation mainly occurred in form of dust. Small meteorites were, nevertheless, formed as well, but their distribution shows that they were basically produced in the main fragmentation, which occurred at 28 km.

Bunburra Rockhole

The reported meteorite fall occurred over SW Australia on July 20, 2007. The event was instrumentally recorded by the Desert Fireball Network (Spurný et al. 2009). It is the fifth event, for which the meteorite fall and its location were successfully predicted based on fireball data, and the first one was based only on data from dedicated instruments. Three meteorites (masses of 174, 150, and 15 g) were found in the predicted fall area. Bunburra Rockhole meteorite is classified as an anomalous basaltic achondrite (Bland et al. 2009). It is the first known meteorite from Aten type orbit, the first achondrite with known orbit, and the first instrumentally observed meteorite fall in the southern hemisphere (Spurný et al. 2009).

This meteorite fall was produced by a relatively small meteoroid, which caused not so bright a fireball with a terminal height of 30 km. The initial mass of the meteoroid was about 22 kg. This value results from an application of the gross-fragmentation model (Ceplecha et al. 1993) and the same value was also obtained by the more sophisticated FM model (Ceplecha and ReVelle 2005), which gave almost identical solution. The meteoroid entered the atmosphere with a low speed of 13.4 km s^{-1}, and the maximum absolute (100 km distance) brightness of −9.3 magnitudes was reached after a very steep increase, surprisingly near the beginning at an altitude of 54.8 km. After a small decrease, it stayed almost constant near the end, where three smaller flares were observed (Spurný et al. 2009, 2011). The terminal speed was estimated as 5.7 km s^{-1}. Based on these data, the apparent strength at the first fragmentation ($H \sim 54.8$ km) may be estimated as about 0.1 MPa. The apparent strengths at lower altitudes (31–38 km) are estimated as about 0.74–0.9 MPa (Table 4) (Spurný et al. 2011).

Almahata Sitta

On October 6, 2008, a small asteroid, 2008 TC_3, was discovered, and precise orbital parameters indicated imminent collision with the Earth (Jenniskens et al. 2009). The entry of the body into the Earth's atmosphere on October 7, 2008, over Sudan with velocity 12.42 km s^{-1} was recorded by satellite systems, including Meteosat 8 (Borovička and Charvat 2009) and infrasound stations (Jenniskens et al. 2009). Meteorite search allowed collectors to find about 300 fragments with total mass up to 3.95 kg (Jenniskens et al. 2009). Masses (from 1.5 to 283 g) were found along a 29 km path.

Almahata Sitta was classified as an anomalous polymict ureilite (Jenniskens et al. 2009). It is an unusual and intriguing case. Different lithologies, including a number of nonureilite fragments (enstatite and ordinary chondrites), were found among retrieved samples. All pieces are fresh and unweathered, and so would probably have been incorporated into asteroid 2008 TC_3 and did not originate from an earlier strewn field (Bischoff et al. 2010a). This indicates that the asteroid was probably a collection of different lithologies, which suggests an

object more like a rubble pile than a fractured breccia. A puzzle, however, is that the asteroid's pre-entry lightcurve gave a rotation rate too fast for a cohesionless rubble pile (Jenniskens et al. 2009). The measured bulk density of Almahata Sitta fragments varies from fragment to fragment, and is about 2.9–3.1 g cm^{-3} and porosity about 15–20% (Kohout et al. 2010, 2011) close to the typical ureilite values (3.05 g cm^{-3} and 9%, Britt and Consolmagno 2003). The pre-atmospheric density of the bulk object, however, was probably less. For example, Welten et al. (2010) estimated the macroporosity of the asteroid as high as about 50%. One small piece of Almahata Sitta was disrupted in the laboratory and its measured tensile strength was about 56 ± 25 MPa (Jenniskens et al. 2009).

Initial diameter of this meteoroid was estimated as 4.1 ± 0.3 m based on asteroid visual magnitude (Jenniskens et al. 2009). Corresponding pre-atmospheric mass (if $\rho = 2.3$ g cm^{-3}) is about 83 ± 25 t (Jenniskens et al. 2009). This estimate correlates well with the mass obtained based on infrasound signal (87 ± 27 t). The irradiated energy recorded by US DoD satellites allows estimating initial mass as 56 t assuming the integral luminous efficiency 9.3% based on optical events calibrated by infrasound registration (Brown et al. 2002b). Accordingly, theoretic estimates (Nemtchinov et al. 1997) that the integral luminous efficiency is slightly lower for this low velocity entry (6.8–8.2%), and these values result in initial mass of about 63–77 t. We will assume 70 t as current best estimate of the initial mass.

Analysis of Meteosat 8 images (Borovička and Charvat 2009), description of the light curve (Jenniskens et al. 2009), and modeling efforts (Popova 2010) suggest that massive dust release due to meteoroid breakup occurred at altitudes 44, 37, and possibly at 53 km. The breaking pressures were estimated as 0.2–0.3 MPa (at 46–42 km altitude) and 1 MPa (at 33 km; Jenniskens et al. 2009). We will assume apparent strengths as 0.3, 0.9, and 1.3 MPa. As a result of the apparent massive dust release, the recovery of only a tiny fraction of the mass, the different lithologies of rocks, and the rotational evidence against a cohesionless rubble pile, we suggest the object was weakly bonded by some fine-grained matrix material that was lost during the fragmentation events. Such material might be generated in a regolith layer, perhaps weakly cemented by bits of impact.

Jesenice

The Jesenice meteorite fall occurred on April 9, 2009, in Slovenia. The fireball was detected by two stations of the EN in the Czech Republic, three low-resolution cameras in Slovenia, and 15 seismic stations in Austria, Slovenia, and Italy (Spurný et al. 2010). Three meteorites with a total mass of 3.6 kg were found and classified as L6 ordinary chondrites (Bischoff et al. 2010b).

Noble gas neon ratio estimates (Ott et al. 2010) suggested an initial meteoroid radius >0.3m, corresponding to an entry mass about 384 kg for a spherical meteoroid. The radius estimate based on radionuclide production is smaller, <0.2 m (Bischoff et al. 2010b) that corresponds to an initial mass of about 113 kg.

The modeling of the light curve and seismic records of the fireball yielded the initial mass of the meteoroid (170 ± 80 kg) and its fragmentation sequence. At a height of 46 km, under the ram pressure of 0.3 MPa only, the meteoroid fragmented into six nearly equal parts. Five of these pieces fragmented again between heights 26.5 and 23 km and ram pressures of 3.5–3.9 MPa. The remaining piece survived 3.9 MPa without fragmentation, but disrupted later at a height 19.5 km under 3.2 MPa.

Grimsby

The Grimsby meteorite fall was recorded by the multi-instrumental Southern Ontario Meteor Network on September 26, 2009, in Southern Ontario, Canada. It registered on six all-sky video cameras, a large format CCD, infrasound station, and HF meteor radar (Brown et al. 2011). In addition, meteorite fragments falling during dark flight were recorded by Doppler weather radars. Thirteen meteorite fragments totaling 215 g in mass were collected and classified as H4-6 ordinary chondrites (McCausland et al. 2010; Brown et al. 2011).

Noble gas neon ratio estimates (Cartwright et al. 2010) suggested an initial meteoroid radius >0.4m, corresponding to an entry mass about 960 kg a spherical meteoroid. An initial mass of 33 ± 16 kg was determined from the modeling of the infrasound signal, whereas modeling of the light curve and deceleration predicted a similar best-fit initial mass near 27 kg, with an upper limit <100 kg (Brown et al. 2011).

The Grimsby fireball shows signs in its lightcurve and in radar data of fragmentation beginning near 70 km height, with intense fragmentation starting near 45–50 km height. At these heights, the meteoroid experienced ram pressures between 0.03 and 0.3 MPa. The major fragmentation at 39 km occurred under 1.5 MPa, later major fragmentations at 33 and 30 km altitude occurred at 3.2 and 3.6 MPa, respectively (Brown et al. 2011).

SUMMARY OF 13 METEORITE FALLS

We collected data about 13 meteorite falls with detailed observational data and known orbital parameters. These meteorites include nine ordinary

chondrites of different types, three achondrites, and one carbonaceous chondrite (Table 2). Their bulk densities are in the range 1.64–3.59 g cm^{-3}, and their microporosities vary from 0 to approximately 40%. These bodies entered the atmosphere with velocities 12.4–22.5 km s^{-1}, and corresponding fireballs had the brightness of about −9.3 to −22 magnitudes.

The initial meteoroid masses ranged from 22 to 70,000 kg. Their orbits suggest origins in various parts of the Main Belt of asteroids.

Fragmentation data for the cases under consideration are collected in Table 4. Mass and velocity estimates are given along with strength estimates at breakups. It should be noted that the best observational values of mass at breakup listed are not very precise (see the Comments on Meteoroid Mass Estimates section). In the worst cases, the uncertainties may reach half an order of magnitude. Ram pressures are known better in most cases (the precision of estimates are about 10–30%).

To proceed further, we have to look at the fragmentation history of individual meteoroids. In all cases, the fragmentation proceeded in several steps. The correlation of apparent bulk strength (or ram pressure at the time of failure) of the meteoroid (Table 4) with its mass at different breakups is shown in Fig. 4. In most cases, the first breakup occurred under the ram pressure lower than 1 MPa (Fig. 4). This first breakup had the form of either the separation of relatively small fragment(s) from the main body (Příbram, Innisfree, Park Forest), losing about half of the mass (Lost City), or severe disruption of the body creating fragments in an order of magnitude smaller than the original mass (Peekskill, Morávka). Even in the cases when fragmentation below 1 MPa was not observed (Neuschwanstein, Villalbeto de la Peña), this may be because of paucity of data and not because of a real lack of produced small pieces. In some cases, the following breakups occurred under increasing ram pressures. In other cases, however, the last breakups of the smallest pieces occurred under lower pressures than the previous breakups (Lost City, Morávka, Peekskill). It is plausible that a violent breakup might produce fracture networks that result in some remaining portions of the body being even weaker. Typically, the maximum encountered loading pressure found is in the range of 5–10 MPa. In none of the 13 cases was 9.6 MPa exceeded without fragmentation. After that, the ram pressure decreased because the daughter fragments were quickly decelerated. They either survived intact or fragmented under lower pressures. In the Innisfree and Lost City cases, both with low initial mass, the pressure never reached 5 MPa. After several fragmentations, the remaining piece was not large enough to be able to reach dense atmospheric layers without severe deceleration. Peekskill, on the other hand, did not reach dense layers because of extremely shallow trajectory. Only in the cases of Tagish Lake and Almahata Sitta, 5 MPa was not reached because of low strength of the bodies.

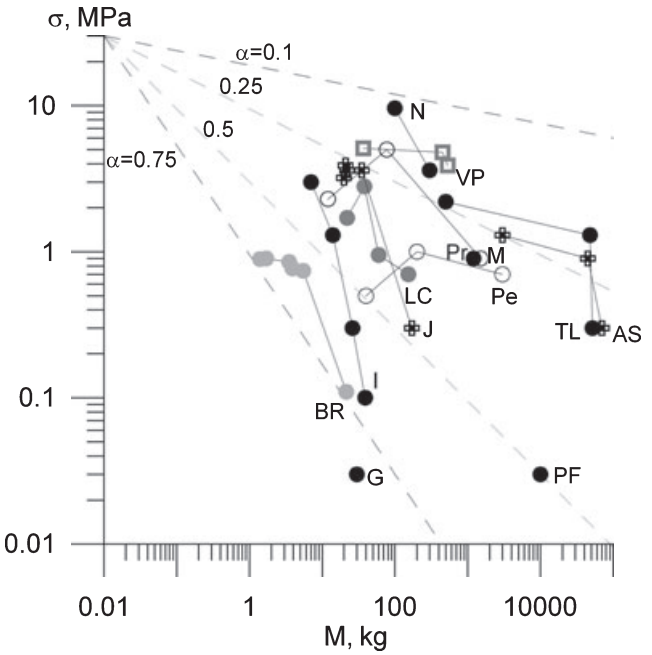

Fig. 4. Estimated apparent bulk strength (= ram pressure in Table 4) at first, second, and third breakups as a function of mass for our 13 cases (Pr—Příbram; LC—Lost City; I—Innisfree; Pe—Peekskill; TL—Tagish Lake; M—Morávka; N—Neuschwanstein; PF—Park Forest; VP—Villalbeto de la Pena; BR—Bunburra Rockhole; AS—Almahata Sitta; J—Jesenice; G—Grimsby). In some cases, other breakups predated the first listed breakup. In the case of Peekskill, for example, there is evidence of breakup before our first observed event. The dashed lines represent power law function, which relates laboratory strength data to bulk rock strength data.

ARE THE FALLS REPRESENTATIVE?

The 13 observed meteorite falls still represent a relatively small sample, in particular, when we consider that data for some of them are not very precise. Before proceeding with the analysis, we therefore examine the question of whether the class of objects we are studying is representative of most bolides or perhaps statistically anomalous. Are the conclusions drawn from bolides that disintegrate and drop numbers of recoverable rocks really representative? The process of fragmentation generally produces one or more bright flashes, and one might suggest that such objects are more likely to be photographed by bystanders than objects that do not break up. Besides, the chance of recovery is higher when many fragments land. So, the meteoroids that fragmented heavily may be over-represented in the sample of recovered meteorites. We therefore included in

our analysis other observed fireballs. First, we included 13 largest fireballs observed by the European Network (Table 5). Second and third, to extend the mass range of our sample, we also considered the atmospheric fragmentation of smaller meteoroids studied by Ceplecha et al. (1993) and several large meteoroids observed on global scale by satellites.

European Network Bolides

We collected 13 photographic records of type I (or close to type I) big fireballs observed by the European network (Table 5). Group I bodies are of the smallest ablation ability and of the greatest bulk density, group II fireballs belong to meteoroids of somewhat lower density and greater ablation ability (Ceplecha et al. 1998). Group I was proposed to be connected with ordinary chondrites, and type II fireballs tentatively belong to carbonaceous bodies (Ceplecha et al. 1998). For all, fireballs radiometric light curves are also available, where at least main features are reliably visible. We collected all such cases (13 bolides) recorded by EN during this century, 11 of them are type I, one belongs to type II, and one may be classified as type I/II. Light curves of these bolides demonstrate flares mainly in the middle or end part of trajectory (nine cases). In three cases, light curves have no well-produced maximum, although many flares were recorded (Table 5).

This table contains one of our 13 cases under study (Neuschwanstein), but at least three other cases from Table 5 (Vimperk, Turji-Remety, and Martin) had significant terminal mass and predicted meteorite fall (unfortunately not found). Initial masses of these meteoroids were estimated to be in the range 27–4300 kg, which is similar to our data set.

In all cases, bright flashes—presumed fragmentation events—were observed along the track. The first fragmentation event was above 34 km (for all cases except one), corresponding to estimated low bulk strengths of 0.2–3.6 MPa (Table 5). The lowest first breakup was observed for Turji-Remety bolide at 29 km altitude under loading 5.9 MPa, but its light curve was observed from great distance and only main features were visible. These estimates are in the same range as our data (0.1–3.6 MPa; Table 3). Maximal dynamic loading for EN bolides are 0.5–11.8 MPa (Table 5) and again are close to the data of Table 3 (2.2–9.6 MPa). It is interesting to note that for two known or probable meteorite-producers (Neuschwanstein and Turji-Remety), observed ram pressure is significantly higher (in all parts of trajectory) than for all remaining cases from both tables. It would infer significantly stronger material than for remaining bodies, in which case our study may be somewhat biased toward stronger samples.

Prairie Network Fireballs

Of 30 fragmenting fireballs analyzed by Ceplecha et al. (1993), 28 fragmented under 1 MPa and the other two below 1.2 MPa. Ceplecha et al. (1993) also observed 21 nonfragmenting fireballs (although some of them may have encountered less severe fragmentation not recognizable by the dynamic method). Only four of them, however, encountered pressure up to 1.5 MPa and only one survived 5 MPa without fragmentation. The fragmentation of small meteoroids (< 10–100 kg) is therefore the rule rather than the exception.

Data on apparent strength versus mass at the fragmentation for 17 PN bolides are presented in Fig. 5. These fragmentation data were obtained courtesy of Dr. Zdenek Ceplecha. All these bolides were included in the data sample studied by Ceplecha et al. (1993) and were classified as bolides with one fragmentation point, which was well determined using dynamical gross-fragmentation method. Masses at breakup were estimated as 0.026–34 kg mainly, with two larger bodies (163 and 263 kg). Altitudes of disruption were above 38 km altitude and corresponding apparent strength may be estimated as 0.1–1 MPa. All these meteoroids were classified as type I and type II bodies.

Satellite Network Bolides

Satellite Network (SN) observations estimated the entry velocity for several recorded events. For this group, we rarely were able to study the whole fragmentation history, but only the main fragmentation. We estimated the apparent strength of these meteoroids to compare them with our main data set. The mass of meteoroid 1 February 1994 was estimated as 400,000 kg (Nemtchinov and Popova 1997), the body entered the atmosphere with the velocity of about 24 km s^{-1} (Tagliaferri et al. 1995). On the basis of modeling results, we may roughly estimate the apparent strength as approximately 0.5–1 MPa at 50 km altitude and approximately 10 MPa at 30 km altitude. The initial mass and velocity of St. Robert meteorite (June 15, 1994) were estimated as 1200–2000 kg and 12.7–13.3 km s^{-1} (Brown et al. 1996). The meteoroid was probably broken at the altitude 37 km under ram pressure of about 0.9 MPa. The El Paso bolide was registered on October 9, 1997. Its initial velocity and mass were estimated as 25 km s^{-1} (Hildebrand et al. 1999) and 8000 kg (Popova and Nemchinov 2008). Corresponding apparent strength at breakup at 28–30 km altitude is about 5–10 MPa, we will adopt 7.5 MPa. Greenland bolide (December 9, 1997) entered the atmosphere with high velocity approximately 30 km s^{-1} (Pedersen et al. 2001) and revealed several fragmentation events at altitudes of

Table 5. Data on the largest European Network (EN) bolides (mostly of type I, which could produce a meteorite fall).

											First fragmentation			Last fragmentation			
EN fireball	Name	Date	M_∞ (kg)	M_E (kg)	Mag max.	V_∞ (km s^{-1})	H_B (km)	H_E (km)	ZR (°)	PE/type	V (km s^{-1})	H (km)	P (MPa)	V (km s^{-1})	H (km)	P (MPa)	Comments
EN270200	Senohraby	02/27/2000	3.6	0.3	−10.0	18.79	80.1	31.6	27.0	−4.40/I	17.3	46.5	0.45	16.0	42.0	0.7	WPM-M, first fragm. = max. brightness. Still earlier small flare at 62 km under P = 0.08 Mpa
EN310800	Vimperk	08/31/2000	105.	5.	−13.8	14.92	81.8	21.5	47.6	−4.29/I	13.2	34.4	1.7	9.9	25.9	3.5	WPM-E, periodic fluctuations in first half of LC
EN171101	Turji-Remety	11/17/2001	4300	450.	−18.5	18.48	81.4	13.5	50.4	−4.27/I	16.9	29.0	5.9	13.6	21.9	11.8	WPM-ME, radiometric light curve from 650 km! distance, only main features visible
EN060402	Neuschwan-stein	04/06/2002	300.	20.	−17.2	20.95	85.0	16.0	40.5	−3.98/I	19.7	34.0	3.6	11.4	20.8	9.6	WPM-E, still smaller flares earlier and one larger in between
EN170702	Jesenik	07/17/2002	5.	0.3	−9.0	20.73	87.1	30.1	43.5	−4.15/I	–	–	–	18.0	39.2	1.6	WPM-ME, lower resolution LC, only main features visible
EN250203	Kacov	02/25/2003	2.8	0.1	−7.0	13.94	74.1	33.9	62.6	−4.34/I	13.1	49.0	0.2	11.1	40.7	0.4	WPM-M, four main flares, max. flare at 43.5 km under P = 0.3 MPa
EN290903	Oświęcim	09/29/2003	72.	0.04	−14.7	23.09	89.4	30.5	50.3	−4.52/I	22.9	59.1	0.2	15.0	32.0	3.1	WPM-E, low-resolution LC, only main features visible, first fragmentation indistinct
EN291103 B	Chotebor	11/29/2003	11.	0.01	−11.6	28.06	82.7	36.4	26.2	−4.66/I or II	–	–	–	26.6	52.9	0.5	WPM-BM, only one main dubbed flare near middle of LC rather toward beginning

Table 5. *Continued.* Data on the largest European Network (EN) bolides (mostly of type I, which could produce a meteorite fall).

											First fragmentation			Last fragmentation			
EN fireball	Name	Date	M_∞ (kg)	M_E (kg)	Mag max.	V_∞ (km s^{-1})	H_B (km)	H_E (km)	ZR (°)	PE/type	V (km s^{-1})	H (km)	P (MPa)	V (km s^{-1})	H (km)	P (MPa)	Comments
EN100704	Munich	07/10/2004	28.	0.1	−12.6	32.21	85.8	33.2	67.7	−4.02/I	31.8	63.1	0.25	29.8	49.0	1.2	NWPM, many flares of similar intensity
EN280506	Legnica	05/28/2006	65.	0.05	−11.4	17.58	88.0	30.5	58.7	−4.59/I	16.7	46.3	0.5	14.3	37.0	1.2	NWPM, many flares of similar intensity, periodic fluctuations in first half of LC
EN231006 A	Zdiar	10/23/2006	11.	0.2	−11.3	28.86	78.3	26.1	33.0	−3.90/I	28.1	48.6	1.0	27.1	42.6	2.0	NWPM, many flares of slowly increasing intensity
EN040207	Breclav	02/04/2007	500.	0.	−18.0	22.01	84.2	30.6	17.8	−5.17/II	21.8	47.7	0.6	20.5	36.2	2.8	WPM-E, three significant flares with strong terminal flare
EN300807	Martin	08/30/2006	26.	7.	−11.0	16.66	72.9	27.0	39.9	−4.41/I	16.6	67.0	0.04	10.9	29.3	2.5	WPM-ME, periodic fluctuations in first half of LC

Note: WPM-B, -M, -E = well-pronounced maximum, i.e., fireball with significant flare—B near beginning, M near middle and E near end of trajectory; NWPM = not well-pronounced maximum, i.e., fireball without significant flare(s); LC = light curve; M_∞ and M_E = initial and terminal mass; Mag max. = maximum absolute magnitude; V_∞ = initial velocity; H_B and H_E = beginning and terminal height; ZR = zenith distance of radiant; P = ram pressure.

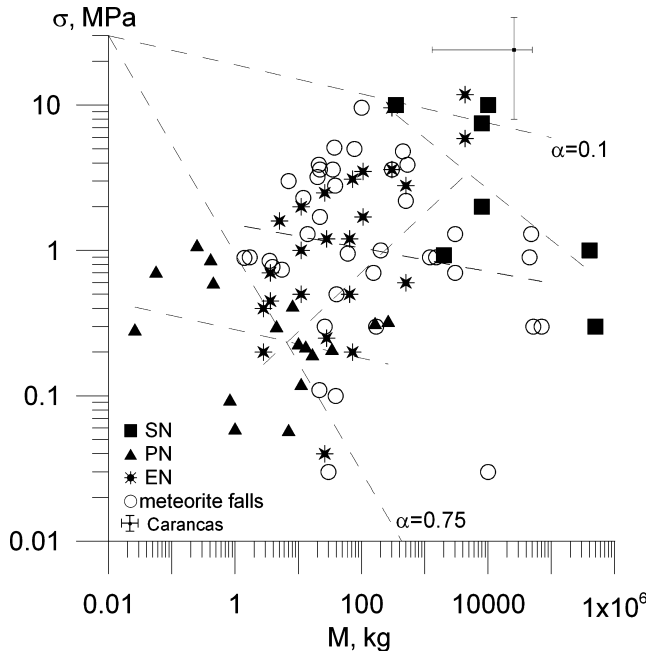

Fig. 5. Estimated apparent bulk strength (as in Fig. 4) supplemented by additional data from Prairie, European, and Satellite Networks. Note that the Prairie Network apparent strength data for predominantly small meteorites are in the same order as the apparent strength of larger meteoroids. The dashed lines represent power law function that relates laboratory strength data to bulk rock strength data, and regression curves obtained for different data sets. The estimate for crater-producing Carancas event (see text) is also given.

about 55–26 km. Meteoroid mass was estimated as 36,000 kg (Pedersen et al. 2001) or 8000 kg (Popova and Nemchinov 2008). We assume the last estimate. Corresponding apparent strength is about 0.4–0.6 MPa at initial breakup and about 10 MPa at lower breakup. The entry of large meteoroid with velocity $V \sim 15$ km s^{-1} was registered in the Pacific Region on January 14, 1999 (Pack et al. 1999). Its mass was estimated as 500,000 kg and apparent strength as < 0.3 MPa (Popova and Nemchinov 2008).

The main fragmentation of large satellite-observed fireballs representing > 1000 kg objects falls nearly in the same pressure range (0.3–10 MPa) as the meteorite falls (Fig. 5). The masses of both groups overlap. In fact, Tagish Lake, Park Forest, Morávka, and Almahata Sitta were observed by satellites as well. Note that the accuracy of satellite data is limited and exact mass and velocity at the point of fragmentation are not well known. We used the best available velocity and mass estimates. Nevertheless, this uncertainty cannot change the fact that the fragmentation pressures of the largest observed fireballs are in the same range as for the smaller ones. This suggests that our sample of 13 cases is reasonably representative.

Carancas and Tunguska

The recent fall of the Carancas stony meteorite in Peru (September 15, 2007) caused the formation of a 13 m wide impact crater. This meteoroid probably did not experience significant atmospheric fragmentation (Borovička and Spurný 2008), although there was no detail observational data. It was classified as ordinary chondrite H 4–5 (Connolly et al. 2008). The meteoroid probably had initial size about 0.9–1.7 m (i.e., $M \sim 1300$–$10{,}000$ kg), and mass at the impact was estimated as 900–4000 kg (Borovička and Spurný 2008). Borovička and Spurný (2008) suggested that the Carancas meteoroid survived atmospheric loading if its strength was 20−40 MPa, and concluded that Carancas was a rare example of a monolithic meteoroid that was free of internal cracks. Kenkmann et al. (2009) derived lower estimates of the Carancas meteoroid strength (12–18 MPa) for vertical impact of 2000–4000 kg body (entry velocity $V \sim 14$ km s^{-1}), as they found that impact velocity as low as approximately 0.6 km s^{-1} was sufficient to produce the crater. These authors, however, preferred the shallow impact possibility (entry angle $< 20°$ from horizon), which allowed decrease of maximal loading along trajectory down to 8–12 MPa or even below (Kenkmann et al. 2009). These values of loading pressure are close to our estimates mentioned above, but this scenario required much larger initial meteoroid mass of 10,000–50,000 kg. The Carancas event confirms that meteoroid strength can vary significantly from case to case. However, it should be noted here that small crater formation on the Earth is an extremely rare event due to disruption of meteoroids in the atmosphere, given that 10–30 similar sized bodies enter the atmosphere every year (Nemtchinov et al. 1997; Brown et al. 2002b). The estimate for Carancas meteoroid is shown in Fig. 5.

In contrast to Carancas, much larger objects may also have fractured or rubbly weak structure, although they penetrate quite deep into the atmosphere. The Tunguska 1908 meteoroid, for example, could have had low bulk strength, but because of its large size, it penetrated further into the atmosphere without visually apparent breakup, exploding at a low altitude of about 8 km. Shuvalov and Artemieva (2002) modeled it successfully as a 60 m diameter, zero-strength "liquid-like" mass entering the atmosphere.

Total Data Sample

From above data, we conclude that our 13 cases of observed bolides with meteorite recovery do not represent an unusual class of bolides. The picture arising from our study is that the meteoroids of asteroidal origin in the

mass range 0.1–10^5 kg (size range 0.02–4 m) start to fragment under similar low pressures of 0.1–1 MPa. There may be exceptions, which survive up to several megapascals. If there is enough mass to reach dense atmospheric layers with large velocity, loading pressures of 5–10 MPa are typical to cause further severe breakups. Approximately 10 MPa seems to be the upper limit of strength during any observed breakup of meteoroid material larger than about 1 kg. The Turji-Remety fragments (of about 100 kg) probably survived 10 MPa without fragmentation, but we have not observed any meteoroid that would survive larger pressure except probably Carancas. To produce hundred-kilogram stony meteorites, low initial velocity and shallow trajectory are needed to allow enough time for deceleration.

Although we have limited this article to the 13 known fireballs with recovered meteorites, we note in passing that some other fireballs have displayed even weaker strengths than we have noted here. A typical example is Šumava, which fell in 1974 and exploded in several bursts at altitudes between 76 and 67 km, leaving no known fragments (Borovička and Spurný 1996). Fragmentation pressures or bulk strengths were estimated at only 0.025–0.14 MPa (Nemtchinov et al. 1999). On the basis of low strength, the object was suggested to be possibly of cometary origin, although the pre-encounter orbit was not strongly cometary. The initial mass was of about 5000 kg (Borovička and Spurný 1996).

COMPARISON WITH METEORITE SAMPLE STRENGTH

Published laboratory "intact" meteorite strength measurement data are scarce and are compiled in Table 6. The shock stage classification is listed as used in the original papers. Unfortunately, shock grade information is not given in the meteorite databases for many older finds.

Although there is a considerable spread, it is very clear that tensile strengths are much lower than compressive strengths for the same material. The average compressive strength value is 217 ± 134 MPa, and the average tensile strength is 30 ± 17 MPa. The laboratory strength measurements depend on whether the sample was subjected to a confining pressure, whose meaning may not be entirely clear in some reports. The Morh–Couloumb theory for geological materials predicts that the ratio of unconfined compressive strength σ_c to the unconfined tensile strength σ_t is dependent on the angle of internal friction φ: $\sigma_c/\sigma_t = \tan^2(\varphi/2 + \pi/2)$ (Jaeger et al. 2007). If φ is 35–45°, the ratio is about 4–6, i.e., in the same range as the listed meteorite data within the great scatter. The strength essentially varies among meteorites of the same class (cf. for example L5 chondrites Tsarev and Elenovka; Table 6) probably due to different structure. Samples of Elenovka (fall, 1951) demonstrated very friable structure and as a consequence show the lowest tensile strength (2 MPa) among six studied meteorites in Medvedev et al. (1985). Strength varies also among pieces of the same meteorite (Tsarev, fall 1922, collected in 1979), and decreases for more weathered pieces according to Medvedev et al. (1985). Besides, according to Yamaguchi (1970), it appears that 10 or more test pieces are required to determine the probable true value and the probable true distribution of the strength of the rock. We suspect that many reported meteorite sample strengths are based on small numbers of tested sample.

The data set is too small to allow conclusions about correlation of strength with meteorite type or shock stage. It should be noted here that the typical mass of the measured samples is about 10–30 g, which is much smaller than the mass of the meteoroids we consider.

The only strength measurement of one of our studied 13 meteorites was done by Jenniskens et al. (2009). Tensile strength of Almahata Sitta small piece (1.5 g) appeared to be in the same range: 56 ± 25 MPa (Jenniskens et al. 2009). During the entry, the meteoroid was broken under the loading smaller 1 MPa (Tables 3 and 4).

All observed atmospheric fragmentations (Tables 3 and 4) occurred under much lower ram pressures than the measured compression and tensile strengths of meteorite samples, with the exception of the tensile strengths of Elenovka (2 MPa, very friable body) and Peace River (6 MPa) meteorites.

OBSERVED RELATION BETWEEN STRENGTH AND MASS

According to the statistical strength theory (Weibull 1951) and direct observations on natural rocks (e.g., Hartmann 1969), the strength of a body in nature tends to decrease as body size increases. This may seem counter-intuitive, but in the course of natural processes larger volumes are likely to develop fractures or microfractures. The effective strength is usually expressed as

$$\sigma = \sigma_s (m_s/m)^{\alpha}, \quad (2)$$

where σ and m are the effective strength and mass of the larger body, σ_s and m_s are those of small specimen, and α is a scaling factor. The values of the scaling factor vary over a wide range, depending on the terrestrial material examined (see references in Asphaug et al. 2002). It has not been proven that these values hold for meteorite strength, though it is commonly assumed in meteoroid

Table 6. Meteorite sample strengths.

No.	Class	Shock stage	Meteorite	Compression strength (MPa)	Tensile strength (MPa)
1	LL3	S3	Krymka	160[c]	22[c]
2	L5	e–f (~S6[a])	Elenovka	20[c]	2[c]
3	L5	e–f	Tsarev	157, 222, 450, 420[c,d]	16, 26, 55, 62[c,d]
4	L5	e	Kunashak	265[c]	49[c]
5	L5	e	Arapahoe	358[d]	
6	L5	S4	La Lande	381[d]	
7	L5	–	Homestead		34[e]
8	L6	S2	Holbrook	63[d,e]	
9	L6	–	Ness County	84[d]	
10	L6	S5	Kyushu	98[c]	11[c]
11	L6	S3–5	Mocs		26[e]
12	L6	S4	Bruderheim		31[e]
13	L6	S3[b]	Peace River		6[e]
14	H3	S1	Dhajala		26[e]
15	H5	S2–3	Jilin		42[e]
16	H5	S3	Pułtusk	213[c]	31[c]
17	H5	–	Covert	77[d]	
18	H5	S3	Alamogordo	274[d]	
19	H6	–	Morland	163[d]	
20	H6	–	Kimble County	327[d]	
21	CV3[g]	–	Allende		28[e]
22	CO3[g]	–	Kainsaz		31[e]
23	Mesosiderite	–	Łowicz		37[e]
24	H4–H6(?)	–	Seminole	173[f]	22.5[f]

Source: [a]Migdisova and Zaslavskaya (1984); [b]Chen et al. (1996); [c]Medvedev et al. (1985); [d]Tsvetkov and Skripnik (1991); [e]Svetsov et al. (1995); [f]Baldwin and Sheaffer (1971). [g]Some carbonaceous chondrites are much weaker and more crumbly than these two examples.

fragmentation theories (e.g., Baldwin and Sheaffer 1971; Nemtchinov and Popova 1997; Borovička et al. 1998; Artemieva and Shuvalov 2001; Bland and Artemieva 2006). The value of exponent $\alpha \sim 0.25$ is most often used in modeling. Most of the modeling efforts are based on this strength scaling law, although empirical values of meteoroid strength were taken into account, for example, in modeling of Martian bolides (Popova et al. 2003). The degree of fragmentation is determined by the assumed meteoroid strength and affects the distribution of cosmic material on the ground, meteorite fall statistics, and strewn field formation on the Earth and other planets (Popova et al. 2003; Bland and Artemieva 2006).

The value of exponent α is not well determined. It is often assumed that the effective strength decreases with size as strength $\sim$ size$^{-0.5}$, which means strength decreases with mass as mass$^{-0.16}$, i.e., $\alpha \sim 0.16$ (Holsapple 2007, 2009). Svetsov et al. (1995) reviewed strength data for meteoroids and suggested that the power α may vary in a wide range from 0.1 to 0.5 and may depend on the projectile size range and material (see also Tsvetkov and Skripnik 1991). Recently, a compilation on strength scaling for intact rock samples 1–200 cm in size (2–30 cm mainly) was published by Yoshinaka et al. (2008). It was found that strength reduction of intact rock due to scale effect occurs in both hard and soft rock, but the trend of change depends on rock type, strength, texture, etc. (Yoshinaka et al. 2008). The exponent power varies in wide ranges of 0.03–0.3, and in some cases, the effect was not observed (Yoshinaka et al. 2008).

The regression function, which can be constructed based on total fragmentation data from Table 4 and Fig. 4, corresponds to the exponent power $\alpha \sim 0.1$. If we include the average value for meteorite strength measurements ($M \sim 0.01$ kg; 30 MPa), the power exponent increases up to $\alpha \sim 0.15 \pm 0.14$, and is statistically significant. However, deviations from the law (2) are evident from Fig. 4. Many breakups late in the sequence occur at lower loading pressure than the earlier fragmentations of the same body. For example, for Morávka, later breakup occurs at 2.3 MPa loading pressure whereas the main breakup occurred at 5 MPa. Recovered Morávka meteorites have a significant part of their surfaces without fusion crust, suggesting fragmentation at velocities below the ablation boundary of 2–3 km s^{-1}, under low loading. It seems that weakly fractured pieces might have been created from more coherent pieces during their loading and breakup events.

The fragmentation history of individual meteoroids for 10 cases is shown in Fig. 4. The slope of corresponding individual fitting curves shows large scatter ($\alpha \sim -0.05 \pm 1.9$). For Almahata Sitta meteoroid, the exponent is about $\alpha \sim 0.27$, if to supplement the flight data by the measured tensile strength for 1.5 g fragment (~56 MPa; Jenniskens et al. 2009).

If we include meteor network data (Fig. 5), we find much larger deviations from the strength scaling law. Prairie Network bolides are disrupted under smaller loading than the strength scaling law predicts. We can see that the fragmentation of < 10–100 kg bodies did not occur at higher pressures than the pressures for larger bodies, as one could expect from the Weibull law (Equation 2). If all mentioned data are combined in the united data set, there is almost no correlation between apparent strength and meteoroid mass. The apparent strength for wide mass range (0.1–10^6 kg) varies in the range 0.1–10 MPa. This fact shows that the difference between the breakup strength of meteoroids and laboratory strength of meteorites is not simply a matter of different size.

Meteoroids over a wide mass range exhibit fragmentation during the entry under similar low pressures, which seems to contradict the Weibull law that larger natural rocks tend to have weaker effective bulk strengths than smaller rocks of the same materials. If correct, this conclusion may also relate to the collisional histories and internal distributions of weaker and stronger fractures produced throughout meteoroids by their collisional origins. For example, as meteoroids are released by impacts suffered by their parent bodies, the small fragments produced close to an impact site may have higher density of small fractures than large fragments from the other side of the parent asteroid. This effect of cratering history may compensate for the usual effects that cause small fragments to be noticeably stronger than big ones.

The meteoroids investigated in this article formed during collisions in space 5–50 Ma, according to the exposure ages in Table 2. They had initial sizes between 0.1 and 4 m before entering Earth's atmosphere (Table 2), and their parent bodies were larger. The collisional fragmentation event that launched our specific meteoroid may not have been the only one in the object's history. The bodies we discuss here, typically of meter or submeter scale, seem too small to have true, zero tensile strength rubble pile structure, but might have spent time as constituents of weakly cemented regolith or rubble piles. In any case, we suggest that most of them suffered collisional histories that left them sufficiently laced with sufficient fractures to produce very low bulk strengths.

We suggest that our result of low bulk strengths of < 5–10 MPa may thus apply to a large percentage of asteroid fragments up to scales of at least 10 m diameter, and possibly up to 100 m. Richardson et al. (2002, p. 512) studied asteroids and concluded on observational and theoretic grounds that many, if not most, kilometer-sized asteroids may have aggregate structure with low tensile strength; our work extends this concept down to decimeter sizes, though direct observations speak against aggregate structures (Pravec and Harris 2000). We also note that for meteoroids larger than approximately 60–100 m, it is hard to verify this effect during entry not only because the events (Tunguska scale and larger) are very rare but also because objects of such large size have inadequate time to separate into widely space discrete pieces during the bolide phase; they impact or explode more or less as single bodies, even if coming apart due to low bulk strength.

Some kilometer-sized asteroids have low bulk density and large estimated macroporosity (Britt and Consolmagno 2001) that support the model of them as rubble pile. The rubble pile concept typically has not been applied to meter-scale objects. Small asteroids such as those observed to enter the atmosphere may be composed of more than one rock. The peculiar Almahata Sitta meteorite probably composes of different lithologies (Bischoff et al. 2010a). If Almahata Sitta is heterogeneous in its lithology, it indicates that aggregate nature may be important at smaller scales. The other known polymict breccia Kaidun survived the atmospheric entry as a single piece (Ivanov et al. 1984). Some pre-entry meter-sized bodies may be aggregates of different types, and others may be weakly coherent blocks of a single rock type, but laced with fractures, so that they fall apart easily upon entry.

Holsapple (2007) considered geological-like materials that have tensile and cohesive strength and estimated maximal possible spin rates of asteroids in dependence on their shape, density, size, and material strength. He found that the presence of small amount of strength allows much more rapid spins. According to his estimates, the maximum observed spin rates of the fastest spinning, small asteroids only require a cohesive size-dependent strength of $2.25R^{-1/2}$ MPa, where R is average body radius (in cm). It means that a 1 m body only requires a cohesive strength of 0.225 MPa to spin as fast as 1 rad s^{-1}, and a 10 m body only 71 kPa to spin at 0.1 rad s^{-1}. These strength values do not contradict our data.

FRACTURES IN METEOROIDS

Strength of Fractured Material

Meteorites are composed of minerals bound together by interlocking of mineral grains or fine-grained cementing

matrix material. A decimeter to meter-sized meteoroid, however, is a discontinuous material, containing joints and other partings, which divide the mass into discrete blocks. It is the fissures and cracks, pre-existing or grown from small fissures or other defects during atmospheric entry, which may largely control the resistance of the body upon atmospheric loading, and not the strength of mineral grains or cementing material (as usually measured in the laboratory). Partings in a meteorite have probably friction coefficients that are similar to slope failure angles in terrestrial rocks.

Under aerodynamic loading during the entry into the atmosphere, the long cracks and even the small-scale fissures may increase their length by propagation due to enhancement of stresses at the sharp/pointed ends of the cracks, eventually reaching the size of the meteoroid and dividing it into fragments. In contrast, even if blocks in the rock are almost completely divided by open cracks or rubbly structure, the heap of these blocks will not move due to friction and geometrically interlocking textures. Shuvalov and Trubetskaya (2010) demonstrated that if the internal friction between fragments is taken into account, the altitude of breakup and deceleration decreases.

Fissures in Fallen Meteorites

To demonstrate that fissures and cracks are indeed present in larger meteoroids, we inspected a set of slabs of large chondrites available at the Natural History Museum, Bern. They are stones from strewn fields, and all contain abundant internal discontinuities. These can be classified into four groups. The first group is characterized by sets of parallel shock veins (Fig. 6a). Such shock veins are commonly dark due to the fluidization of metal and sulfide along these veins, formation of friction glass, and grain size reduction (shock darkening). A second group contains a mesh of nonparallel, but connected shock veins (Fig. 6b). In both groups, sections of these veins are actually hair-like fissures. A third group of meteorites shows widely open cracks of limited length (Fig. 6c). Laterally, these cracks may taper into fissures or closed planar features. In addition to smooth or irregular partings, slickensides (Fig. 6d) and possibly shatter cones built a rare group of observed discontinuities. All these discontinuities and especially the open fissures and cracks dramatically reduce the bulk rock strength of a meteoroid. This is well expressed in the meteorite drill core (Fig. 6e) broken up into several pieces along shock veins. Bulk strength of meter-sized meteoroids is controlled by jointing, and not "intact" rock strength of coherent subunits.

DISCUSSION AND CONCLUSIONS

In all cases where data are available, the bulk strengths upon entry of meteoroids into Earth's atmosphere are much weaker than the strengths of recovered meteorite samples. Bulk strengths of only 0.1 to approximately 1.0 MPa appear typical of the first breakup. This almost certainly reflects a highly fractured state in the parent body, such that the fragments reaching the ground are only the more coherent subunits of a parent body divided by the fractures. We believe that the fractures are consistent with the collision histories inferred for asteroid parent bodies, and in some cases, a rubbly aggregate structure may also decrease the strength of the body. Most Earth-approaching bodies are probably fragments blasted out of larger parents during catastrophic collisional fragmentation events (Heck et al. 2004).

If there is enough mass to reach dense atmospheric layers with large velocity, loading pressures of 5–10 MPa are typical to cause further severe breakups. Approximately 10 MPa seems to be the upper limit of strength observed during breakup of stony meteoroid material larger than about 1 kg. To produce hundred-kilogram stony meteorites, low initial velocity and shallow trajectory are needed to allow enough time for deceleration. In exceptional cases, a meter-sized body may survive 20 MPa and large meteorites or even impact craters may be produced.

We have considered various sources of uncertainty. There are difficulties in determination of fragmentation points (see the Determining the Fragmentation Strength section), and uncertainties in meteoroid mass estimates (see the Comments on Meteoroid Mass Estimates and Evaluation of Individual Cases sections). In some cases, it is difficult to determine what kind of fragmentation is realized—the loss of small amount of mass under breakup (e.g., $< 1\%$) or total disruption into fragments less than a few percent of the initial mass. In consequence, strength estimates are crude in many cases (see discussions in the Comments on Meteoroid Mass Estimates and Determining the Fragmentation Strength sections). As for breakup behavior, there may be additional phenomena besides aerodynamical loading. For example, radiometry with high-time resolution demonstrates numerous millisecond flare events, suggesting additional processes (triboelectricity?), as discussed by Spurný and Ceplecha (2008).

In summary, the strength of a meteoroid, prior to its atmospheric entry, appears to be related to its particular history on its parent body, as well as its taxonomic type. The strength as a function of mass seems to be more or less random, and we are little bit disappointed that

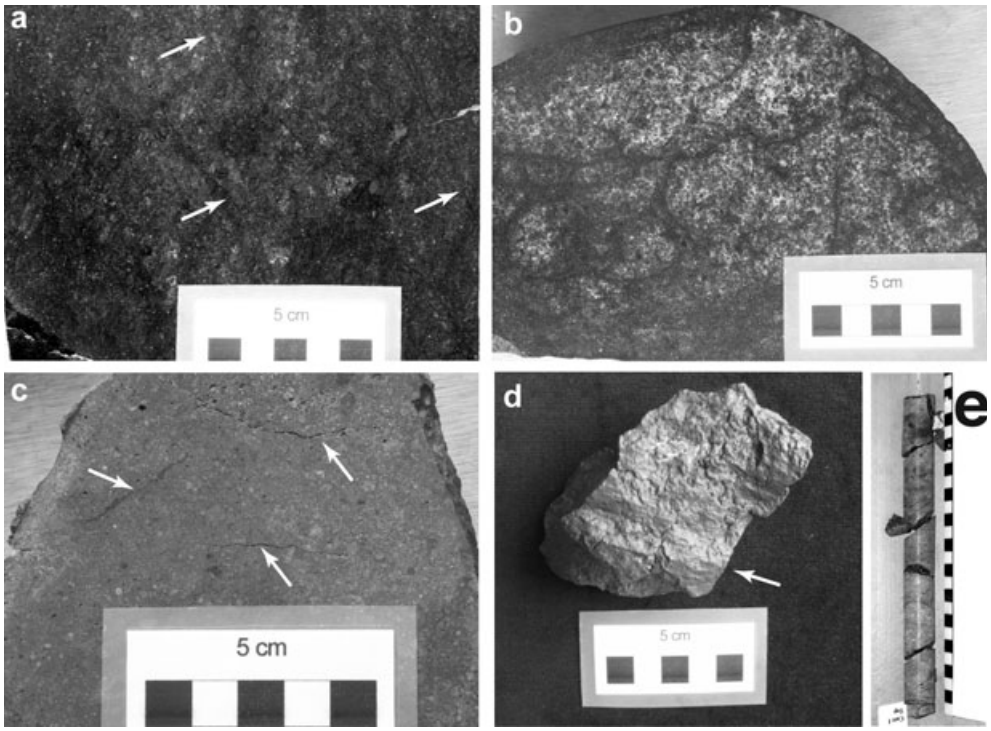

Fig. 6. Examples of partings observed in large chondrites. They all belong to variably sized strewn fields. Fissures and cracks are commonly recognizable in the fusion crust, too. a) Cut and polished slab of Al Huqf (AH) 011. A dominant set of parallel, 2–4 cm spaced shock veins runs from top left to bottom right. These planar features crosscut the stone (20 cm). A second, closer spaced, but less pronounced set of shock veins is intersecting the first at high angle. Irregular fissures stained with metal are well visible on the right. b) Chicken-wire network of shock veins in Sayh al Uhaymir (SaU) 272. Fluidized metal is common in the veins. c) Cut slab of SaU 238. Note that the widely open cracks are not, or only as closed fissures extending to the surface of the stone. d) Slickensides in Jiddat al Harasis (JaH) 275. (e) Dismembered drill core of an approximately 25 cm long JaH 073 sample. Failure of the core due to shear stress from the rotating drill occurred only along the shock vein discontinuities.

we have not found any evident dependence. We, nevertheless, believe that the apparent chaos is not due to bad data or models, but is a natural consequence of the individual collisional history of each individual meteoroid. Probably many meteorites originated in the outer layers of an asteroid, where they suffered impacts and radiation (i.e., gardening) during millions of years, followed by an impact with sufficient energy to eject them from their parent body. More porous objects, e.g., carbonaceous chondrites, may preserve porosity and low density either from initial accretion or associated with the initial fragmentation of the material. The interaction between fragments of disrupted meteoroid (internal friction or other effects) may be the source of additional variations of apparent strength.

Many Earth-crossing asteroids to be visited by robotic or human missions may consist not of single, strong, coherent rocks or metal masses, but rather may be highly fractured. They may thus consist of strong subunits (individual meteoritic rocks) that are weakly bound together. Smaller pieces near the surface may grade into a transitional-regolith-like structure of interlocking fractured pieces, as a result of the surface cratering regime, even if loose regolith has not accumulated. These bolides break up along pre-existing subunits as they enter the atmosphere, and the resulting pieces may fragment further along pre-existing fractures.

There are several implications. First, sample collection may be facilitated by the pre-fractured state. Second, in the long-term future, this may make it more practical to extract samples for possible mineral extraction or "asteroid mining" for human purposes. Third, attempts to interact with hundred-meter-scale asteroids for hazard mitigation may need to take into account low bulk strength and even a possibly crumbly nature. Such a nature could dissipate energy imparted to the body, so that the body might not respond like a coherent rigid body.

The rapidly increasing number of observations in Fig. 1 assures that many of these events, with good trajectories and "ground truth" meteorites, will accumulate in coming years. We suggest that it would be valuable to increase the number of detection and tracking networks. Also, the theoretic tools should be further refined. For example, "ground truth" meteorites

may allow calculated luminous efficiencies to be correlated with specific meteorite compositional classes. Data from such analyses will shed increasing light on properties of small, near-Earth objects.

Acknowledgments— This paper is dedicated to the memory of Zdenek Ceplecha, who passed away December 4, 2009, during our final stages of manuscript preparation. Dr. Ceplecha pioneered work in the area of our research, with the first photography of a meteorite fall, the 1959 Příbram event, which led to the first orbit determination for a meteorite. Dr. Zdenek Ceplecha provided us his data on PN bolides for this paper. The authors of this paper regret to announce that our coauthor, Ivan Nemtchinov, died on March 12, 2010, during the late stages of preparation of this paper. Nemtchinov was our esteemed colleague in this work and was known for his excellent studies in many research areas, including low-temperature plasma, geophysics of strong disturbances, the radiative and gasdynamical effects accompanying the motion of cosmic bodies in the atmosphere, impacts on the Earth and other planets, and consequences of these impacts.

We thank the International Space Science Institute of Bern, Switzerland, for sponsoring team meetings that permitted us to collaborate on this research. We are grateful to Keith Holsapple for very useful and kind review, which raised lots of interesting and serious points.

Editorial Handling—Dr. Donald Brownlee

REFERENCES

Artemieva N. A. and Shuvalov V. V. 2001. Motion of a fragmented meteoroid through the planetary atmosphere. *Journal of Geophysical Research* 106:3297–3310.

Asphaug E., Ryan E., and Zuber M. 2002. Asteroid interiors. In *Asteroids III*, edited by Bottke W. F. Jr., Cellino A., Paolicchi P., and Binzel R. P. Tucson, Arizona: The University of Arizona Press. pp. 463–484.

Babadžhanov P. B. and Kramer E. N. 1968. Some results of investigations of instantaneous meteor photographs. In *Physics and dynamics of meteors*, edited by Kresak L. and Millman P. M. Dordrecht: Reidel. pp. 128–142.

Bagolia C., Bhandari N., Sinha N., Goswami J. N., Lal D., Lorin J. C., and Pellas P. 1980. Multiple fall of Příbram meteorites photographed. 12. Pre-atmospheric size of the Příbram meteorite based on studies of fossil cosmic ray tracks and spallation products. *Bulletin of the Astronomical Institute of Czechoslovakia* 31:51–58.

Baldwin B. and Sheaffer Y. 1971. Ablation and breakup of large meteoroids during atmospheric entry. *Journal of Geophysical Research* 76:4653–4668.

Beech M., Brown P., Hawkes R. L., Ceplecha Z., Mossman K., and Wetherill G. 1995. The fall of the Peekskill meteorite: Video observations, atmospheric path, fragmentation record and orbit. *Earth, Moon, and Planets* 68:189–197.

Bischoff A. and Zipfel J. 2003. Mineralogy of the Neuschwanstein (EL6) chondrite-first results (abstract #1212). 34th Lunar and Planetary Science Conference. CD-ROM.

Bischoff A., Horstmann M., Laubenstein M., and Haberer S. 2010a. Asteroid 2008 TC_3—Almahata Sitta: Not only a ureilitic meteorite, but a breccias containing many different achondritic and chondritic lithologies (abstract #1763). 41st Lunar and Planetary Science Conference. CD-ROM.

Bischoff A., Jersek M., Grau T., Mirtic B., Ott U., Kučera J., Horstmann M., Laubenstein M., Herrmann S., Řanda Z., Weber M., and Heusser G. 2010b. Jesenice (L6)—A recent meteorite fall from Slovenia (abstract #5044). July 26–30, New York, 73rd Meeting of Meteoritical Society.

Bland P. A. and Artemieva N. A. 2006. The rate of small impacts on Earth. *Meteoritics & Planetary Science* 41:607–631.

Bland P. A., Cressey G., and Menzies O. N. 2004. Modal mineralogy of carbonaceous chondrites by X-ray diffraction and Mössbauer spectroscopy. *Meteoritics & Planetary Science* 39:3–16.

Bland P. A., Spurný P., Towner M. C., Bevan A. W. R., Singleton A. T., Bottke W. F., Greenwood R. C., Chesley S. R., Shrbený L., Borovička J., Ceplecha Z., McClafferty T. P., Vaughan D., Benedix G. K., Deacon G., Howard K. T., Franchi I. A., and Hough R. M. 2009. A anomalous basaltic meteorite from the innermost Main Belt. *Science* 325:1525–1527.

Bogard D. D., Clark R. S., Keith J. E., and Reynolds M. A. 1971. Noble gases and radionuclides in Lost City and other recently fallen meteorites. *Journal of Geophysical Research* 76:4076–4083.

Borovička J. and Charvat Z. 2009. Meteosat observation of the atmospheric entry of 2008 TC_3 over Sudan and associated dust cloud. *Astronomy & Astrophysics* 485:1015–1022.

Borovička J. and Kalenda P. 2003. The Morávka meteorite fall: 4. Meteoroid dynamics and fragmentation in the atmosphere. *Meteoritics & Planetary Science* 38:1023–1043.

Borovička J. and Spurný P. 1996. Radiation study of two very bright terrestrial bolides. *Icarus* 121:484–510.

Borovička J. and Spurný P. 2008. The Caranacas meteorite impact—Encounter with a monolithic meteoroid. *Astronomy & Astrophysics* 485:L1–L4.

Borovička J., Popova O. P., Nemtchinov I. V., Spurný P., and Ceplecha Z. 1998. Bolides produced by impacts of large meteoroids into the Earth's atmosphere: Comparison of theory with observations. I. Benesov bolide dynamics and fragmentation. *Astronomy & Astrophysics* 334:713–728.

Borovička J., Spurný P., Kalenda P., and Tagliaferri E. 2003a. The Morávka meteorite fall: 1. Description of the events and determination of the fireball trajectory and orbit from video records. *Meteoritics & Planetary Science* 38:975–987.

Borovička J., Weber H. W., Jopek T., Jakeš P., Randa Z., Brown P. G., ReVelle D. O., Kalenda P., Schultz L., Kucera J., Haloda J., Týcová P., Frýda J., and Brandstätter F. 2003b. The Morávka meteorite fall: 3. Meteoroid initial size, history, structure, and composition. *Meteoritics & Planetary Science* 38:1005–1021.

Britt D. T. and Consolmagno G. J. 2001. Modeling the structure of high porosity asteroids. *Icarus* 152:134–139.

Britt D. T. and Consolmagno G. J. 2003. Stony meteorite porosities and densities: A review of the data through 2001. *Meteoritics & Planetary Science* 38:1161–1180.

Britt D. L. and Consolmagno G. J. 2004. Meteorite porosities and densities: A review of trends in the data (abstract #2108). 35th Lunar and Planetary Science Conference. CD-ROM.

Brown P., Ceplecha Z., Hawkes R. L., Wetherill G., Beech M., and Mossman K. 1994. The orbit and atmospheric trajectory of the Peekskill meteorite from video records. *Nature* 367:624–626.

Brown P., Hildebrand A. R., Creen D. W. E., Pagé D., Jacobs C., ReVelle D., Tagliaferri E., Wacker J., and Wetmiller B. 1996. The fall of the St-Robert meteorite. *Meteoritics & Planetary Science* 31:502–517.

Brown P. G., Hildebrand A. R., Zolensky M. E., Grady M., Clayton R. N., Mayeda T. K., Tagliaferri E., Spalding R., Macrae N. D., Hoffman E. L., Mittlefehldt D. W., Wacker J. F., Bird J. A., Campbell M. D., Carpenter R., Gingerich H., Glatiotis M., Greiner E., Mazur M. J., Mccausland P. J. A., Plotkin H., and Rubak Mazur T. 2000. The fall, recovery, orbit, and composition of the Tagish Lake meteorite: A new type of carbonaceous chondrite. *Science* 290:320–325.

Brown P., ReVelle D. O., and Hildebrand A. R. 2001. The Tagish Lake meteorite fall: Interpretation of fireball physical characteristics. In *Proceedings of the Meteoroids 2001 Conference, 6–10 August, Kiruna, Sweden*, edited by Warmbein B. ESA SP-495. Noordwijk: ESA Publications Division. pp. 497–505.

Brown P. G., ReVelle D. O., Tagliaferri E., and Hildebrand A. R. 2002a. An entry model for the Tagish Lake fireball using seismic, satellite and infrasound records. *Meteoritics & Planetary Science* 37:661–675.

Brown P., Spalding R. E., ReVelle D. O., Tagliaferri E., and Worden S. P. 2002b. The flux of small near-Earth objects colliding with the Earth. *Nature* 420:294–296.

Brown P., Pack D., Edwards W. N., ReVelle D. O., Yoo B. B., Spalding R. E., and Tagliaferri E. 2004. The orbit, atmospheric dynamics, and initial mass of the Park Forest meteorite. *Meteoritics & Planetary Science* 39:1781–1796.

Brown P., McCausland P. J. A., Fries M., Silber E., Edwards W. N., Wong D. K., Weryk R. J., Fries J., and Krzeminski Z. 2011. The fall of the Grimsby meteorite—I: Fireball dynamics and orbit from radar, video and infrasound records. *Meteoritics & Planetary Science* 46:339–363.

Cartwright J. A., Herrmann S., McCausland P. J. A., Brown P. G., and Ott U. 2010. Noble gas analysis of the Grimsby H chondrite (abstract #5236). 73rd Meeting of Meteoritical Society, July 26–30, New York.

Ceplecha Z. 1961. Multiple fall of Příbram meteorites photographed. *Bulletin of the Astronomical Institute of Czechoslovakia* 12:21–46.

Ceplecha Z. 1996. Luminous efficiency based on photographic observations of the Lost City fireball and implications for the influx of interplanetary bodies onto Earth. *Astronomy & Astrophysics* 311:329–332.

Ceplecha Z. and ReVelle D. O. 2005. Fragmentation model of meteoroid motion, mass loss, and radiation in the atmosphere. *Meteoritics & Planetary Science* 40:35–54.

Ceplecha Z., Spurný P., Borovička J., and Keclíková J. 1993. Atmospheric fragmentation of meteoroids. *Astronomy & Astrophysics* 279:615–626.

Ceplecha Z., Brown P., Hawkes R. L., Wetherill G., Beech M., and Mossman K. 1996. Video observations, atmospheric path, orbit and fragmentation record of the fall of the Peekskill meteorite. *Earth, Moon, and Planets* 72:395–404.

Ceplecha Z., Borovička J., Elford W. G., ReVelle D. O., Hawkes R. L., Porubčkan V., and Šimek M. 1998. Meteor phenomena and bodies. *Space Science Reviews* 84:327–471.

Chen M., Wopenka B., Goresy A. El., and Sharp T. G. 1996. High-pressure assemblages in shock melt veins in the Peace River (L6) chondrite: Compositions and pressure–temperature history (abstract). *Meteoritics & Planetary Science* 31:A27.

Connolly H. C., Smith C., Benedix G., Folco L., Zipfel J., Yamaguchi A., and Chennaoui Aoudjehane H. 2008. The Meteoritical Bulletin, No. 93. *Meteoritics & Planetary Science* 43:571–632.

Consolmagno G. J. and Britt D. T. 2004. Meteoritical evidence and constraints on asteroid impacts and disruption. *Planetary and Space Science* 52:1119–1128.

Englert P. 1985. 53-Mn in a slab of the Lost City meteorite (abstract). 16th Lunar and Planetary Science Conference. pp. 215–216.

Fadeenko Yu. I. 1967. Destruction of meteoroids in the atmosphere. *Fizika Gorenija i Vzryva* 3:276–280.

Fireman E. L. and DeFelice J. 1964. Multiple fall of Příbram meteorites photographed. 7. The tritium and argon-39 in the Příbram meteorite. *Bulletin of the Astronomical Institute of Czechoslovakia* 15:113F.

Golub' A. P., Kosarev I. B., Nemtchinov I. V., and Shuvalov V. V. 1996. Emission and ablation of a large meteoroid in the course of its motion through the Earth's atmosphere. *Solar System Research* 30:183–197.

Goswami J. N., Lal D., Rao M. N., Sinha N., and Venkatesan T. R. 1978. Particle track and rare gas studies of Innisfree meteorite. *Meteoritics* 13:481–484.

Graf T., Marti K., Xue S., Herzog G. F., Klein J., Middleton R., Metzler K., Herd R., Brown P., Wacker J. F., Jull A. J. T., Masarik J., Koslowsky V. T., Andrews H. R., Cornett R. J. J., Davies W. G., Greiner B. F., Imahori Y., Mckay J. W., Milton G. M., and Milton J. C. D. 1997. Exposure history of the Peekskill (H6) meteorite. *Meteoritics* 32:25–30.

Halliday I., Blackwell A. T., and Griffin A. A. 1978. The Innisfree meteorite and the Canadian camera network. *Journal of the Royal Astronomical Society of Canada* 72:15–39.

Halliday I., Griffin A. A., and Blackwell A. T. 1981. The Innisfree meteorite fall: A photographic analysis of fragmentation, dynamics and luminosity. *Meteoritics* 16: 153–170.

Hartmann W. K. 1969. Terrestrial, lunar, and interplanetary rock fragmentation. *Icarus* 10:201.

Heck P., Schmitz B., Baur H., Halliday A., and Wieler R. 2004. Fast delivery of meteorites to Earth after a major asteroid collision. *Nature* 430:323–325.

Hildebrand A. R., Brown P., Crawford D., Boslough M., Chael E., Revelle D., Doser D., Tagliaferri E., Rathbun D., Cooke D., Adcock C., and Karner J. 1999. The El Paso Superbolide of October 9, 1997 (abstract #1525). 30th Lunar and Planetary Science Conference. CD-ROM.

Hildebrand A., McCausland P. J. A., Brown P. G., Longstaffe F. J., Russell S. D. J., Tagliaferri E., Wacker J. F., and Mazur M. J. 2006. The fall and recovery of the Tagish Lake meteorite. *Meteoritics & Planetary Science* 41:407–431.

Hildebrand A. R., Milley E. P., Brown P. G., McCausland P. J. A., Edwards W., Beech M., Ling A., Sarty G., Paulson M. D., Maillet L. A., and Jones S. F. 2009. Characteristics of a bright fireball and meteorite fall at Buzzard Coulee, Saskatchewan, Canada, November 20, 2008 (abstract #2505). 40th Lunar and Planetary Science Conference. CD-ROM.

Holsapple K. 2007. Spin limits of solar system bodies: From small fast-rotators to 2003 EL61. *Icarus* 187:500–509.

Holsapple K. 2009. On the strength of the small bodies of the solar system: A review of strength theories and their implementation for analyses of impact disruption. *Planetary and Space Science* 57:127–141.

Ivanov A. V., Ulyanov A. A., Skripnic A. Y., and Konokona N. N. 1984. The Kaidun polymict carbonaceous breccia: The mixture of incompatible types of meteorites (abstract). 13th Lunar and Planetary Science Conference. pp. 393–394.

Jaeger J. C., Cook N. G. W., and Zimmerman R. W. 2007. *Fundamentals of Rock Mechanics*. Malden, Massachusetts: Blackwell Publishing Ltd.

Jenniskens P., Shaddad M. H., Numan D., Elsir S., Kudoda A. M., Zolensky M. E., Le L., Robinson G. A., Friedrich J. M., Rumble D., Steele A., Chesley S. R., Fitzsimmons A., Duddy S., Hsieh H. H., Ramsay G., Brown P. G., Edwards W. N., Tagliaferri E., Boslough M. B., Spalding R. E., Dantowitz R., Kozubal M., Pravec P., Borovicka J., Charvat Z., Vaubaillon J., Kuiper J., Albers J., Bishop J. L., Mancinelli R. L., Sandford S. A., Milam S. N., Nuevo M., and Worden S. P. 2009. The impact and recovery of asteroid 2008 TC_3. *Nature* 458:485–488.

Kenkmann T., Artemieva N. A., Wunnemann K., Poelchau M. H., Elbeshausen D., and Nunes del Prado H. 2009. The Carancas meteorite impact crater, Peru: Geologic surveying and modeling of crater formation and atmospheric passage. *Meteoritics & Planetary Science* 44:985–1000.

Kohout T., Cheron A., Donadini F., Kletetschka G., and Pesonen L. J. 2004. The possible scenarios of the Neuschwanstein meteorite history based on physical properties (abstract #P33A-0999). American Geophysical Union, Fall Meeting, 13–17 December 2004, San Francisco, CA.

Kohout T., Kiuru R., Haloda J., and Britt D. 2010. Restriction on 2008 TC_3 asteroid properties from study of the Almahata Sitta meteorites (abstract). European Planetary Science Congress, 19–24 September 2010, Rome, Italy; EPSC Abstracts, vol. 5, EPSC2010-692

Kohout T., Kiuru R., Montonen M., Scheirich P., Britt D., Macke R., and Consolmagno G. 2011. 2008 TC_3 asteroid internal structure and physical properties inferred from study of the Almahata Sitta meteorites. *Icarus* 212:697–700.

Lavrukhina A. K., Fisenko A. V., and Kolesnikov E. M. 1974. Multiple fall of Příbram meteorites photographed. 11. Preatmospheric size and radiation age of the Příbram chondrite. *Bulletin of the Astronomical Institute of Czechoslovakia* 25:122.

Llorca J., Trigo-Rodríguez J. M., Ortiz J. L., Docobo J. A., García-Guinea J., Castro-Tirado A., Rubin A. E., Eugster O., Edwards W., Laubenstein M., and Casanova I. 2005. The Villalbeto de la Peña meteorite fall: I. Fireball energy, meteorite recovery, strewn field and petrography. *Meteoritics & Planetary Science* 40:795–804.

McCausland P. J. A., Brown P. G., Hildebrand A. R., Flemming R. L., Barker I., Moser D. E., Renaud J., and Edwards W. 2010. Fall of the Grimsby H5 chondrite (abstract #2716). 41st Lunar and Planetary Science Conference. CD-ROM.

McCrosky R. E., Posen A., Schwartz G., and Shao C.-Y. 1971. Lost City meteorite—Its recovery and a comparison with other fireballs. *Journal of Geophysical Research* 76:4090.

Medvedev R. V., Gorbachevich F., and Zotkin I. 1985. Determination of physical properties of stone meteorites from the point of view of their disruption. *Meteoritika* 44:105–110. In Russian.

Migdisova L. F. and Zaslavskaya N. I. 1984. Some peculiarities of the chemical composition of minerals in shock-metamorphized L chondrites (abstract). 15th Lunar and Planetary Science Conference. pp. 544–545.

Nakamura T., Noguchi T., Zolensky M. E., and Tanaka M. 2003. Noble-gas signatures and mineralogy of the carbonate-rich lithology of the Tagish Lake carbonaceous chondrite: Evidence for an accretionary breccia. *Earth and Planetary Science Letters* 207:83–101.

Nemtchinov I. V. and Popova O. P. 1997. An analysis of the 1947 Sikhote-Alin event and a comparison with the phenomenon of February 1, 1994. *Solar System Research* 31:408–420.

Nemtchinov I. V., Svetsov V. V., Kosarev I. B., Golub' A. P., Popova O. P., Shuvalov V. V., Spalding R. E., Jacobs C., and Tagliaferri E. 1997. Assessment of kinetic energy of meteoroids detected by satellite-based light sensors. *Icarus* 130:259–274.

Nemtchinov I. V., Kuzmicheva M. Yu., Shuvalov V. V., Golub' A. P., Popova O. P., Kosarev I. B., and Borovička J. 1999. Šumava meteoroid—Was it a small comet? In *Evolution and source regions of asteroids and comets: Proceedings of IAU Colloquium 173*, edited by Svoren J., Pittich E. M., and Rickman H. Tatranska Lomnica: Astronomical Institute of the Slovak Academy of Sciences. pp. 51–56.

Oberst J., Heinlein D., Köhler U., and Spurný P. 2004. The multiple meteorite fall of Neuschwanstein: Circumstances of the event and meteorite search campaigns. *Meteoritics & Planetary Science* 39:1627–1641.

Ott U., Herrmann S., Haack H., and Grau T. 2010. Noble gases in two meteorites that fell in Denmark and Slovenia in 2009 (abstract #1196). 45th Lunar and Planetary Science Conference. CD-ROM.

Pack D. W., Tagliaferri E., Yoo B. B., Peterson G. E., and Spalding R. 1999. Recent satellite observations of large meteor events. In *Asteroids, comets, meteors 1999*. Ithaca, New York: Cornell University. 48 p.

Pauls A. and Gladman B. 2005. Decoherence time scales for "meteoroid streams." *Meteoritics & Planetary Science* 40:1241–1256.

Pedersen H., Spalding R. E., Tagliaferri E., Ceplecha Z., Risbo T., and Haack H. 2001. Greenland superbolide event of 1997 December 9, 2001. *Meteoritics & Planetary Science* 36:549–558.

Petrovic J. J. 2001. Mechanical properties of meteorites and their constituents. *Journal of Material Science* 36:1579–1583.

Popova O. 2010. Passage of bolides through the atmosphere (abstract). European Planetary Science Congress, 19–24 September 2010, Rome, Italy. EPSC Abstracts, vol. 5, EPSC2010-722.

Popova O. and Nemchinov I. 2008. Bolides in the Earth atmosphere. In *Catastrophic events caused by cosmic objects*, edited by Adushkin V. and Nemchinov I. Dordrecht, The Netherlands: Springer. pp. 131–163.

Popova O., Hartmann W., and Nemtchinov I. 2003. Bolides in the present and past Martian atmosphere and effects on cratering processes. *Meteoritics & Planetary Science* 38:905–925.

Pravec P. and Harris A. 2000. Fast and slow rotation of asteroids. *Icarus* 48:12–20.

ReVelle D. O., Brown P. G., and Spurný P. 2004. Entry dynamic and acoustic/infrasonic/seismic analysis for the

Neuschwanstein meteorite fall. *Meteoritics & Planetary Science* 39:1605–1626.

Richardson D. C., Leinhardt Z. M., Melosh H. J., Bottke W. F. Jr., and Asphaug E. 2002. Gravitational aggregates: Evidence and evolution. In *Asteroids III*, edited by Bottke W. F. Jr., Cellino A., Paolicchi P., and Binzel R. P. Tucson, Arizona: The University of Arizona Press. pp. 501–515.

Rubin A. E. 1994. Metallic copper in ordinary chondrites. *Meteoritics* 29:93–98.

Shuvalov V. V. and Artemieva N. N. 2002. Numerical modeling of Tunguska-like impacts. *Planetary and Space Science* 50:181–192.

Shuvalov V. V. and Trubetskaya I. A. 2010. The influence of internal friction on the deformation of a damaged meteoroid. *Solar System Research* 44:104–109.

Simon S. B., Grossman L., Clayton R. N., Mayeda T. K., Schwade J. R., Sipiera P. P., Wacker J. F., and Wadhwa M. 2004. The fall, recovery, and classification of the Park Forest meteorite. *Meteoritics & Planetary Science* 39:625–634.

Spurný P. and Ceplecha Z. 2008. Is electric charge separation the main process for kinetic energy transformation into the meteor phenomenon? *Astronomy & Astrophysics* 489:449–454.

Spurný P., Heinlein D., and Oberst J. 2002. The atmospheric trajectory and heliocentric orbit of the Neuschwanstein meteorite fall on April 6, 2002. In *Proceedings of Asteroids, Comets, Meteors Conference*, edited by Warmbein B. Berlin, Germany/Noordwijk, The Netherlands: ESA Publications Division. pp. 137–140.

Spurný P., Oberst J., and Heinlein D. 2003. Photographic observations of Neuschwanstein, a second meteorite from the orbit of the Příbram chondrite. *Nature* 423:151–153.

Spurný P., Bland P. A., Borovička J., Shrbený L., McClafferty T., Singelton A., Bevan A. W. R., Vaughan D., Towner M. C., and Deacon G. 2009. The Bunburra Rockhole meteorite fall in SW Australia: Determination of the fireball trajectory, luminosity and impact position from photographic records (abstract #1498). 40th Lunar and Planetary Science Conference. CD-ROM.

Spurný P., Borovička J., Kac J., Kalenda P., Atanackov J., Kladnik G., Heinlein D., and Grau T. 2010. Analysis of instrumental observations of the Jesenice meteorite fall on 9th April, 2009. *Meteoritics & Planetary Science* 45:1392–1407.

Spurný P., Bland P. A., Shrbeny L., Borovička J., Ceplecha Z., Singelton A., Bevan A. W. R., Vaughan D., Towner M. C., McClafferty T., and Deacon G. 2011. The Bunburra Rockhole meteorite fall in SW Australia: Fireball trajectory, luminosity, dynamics, impact position and orbit from photographic and photoelectric records (in press).

Stauffer H. and Urey H. C. 1962. Multiple fall of Příbram meteorites photographed. III. Rare gas isotopes in the Velká stone meteorite. *Bulletin of the Astronomical Institute of Czechoslovakia* 13:106.

Svetsov V. V., Nemtchinov I. V., and Teterev A. V. 1995. Disintegration of large meteoroids in Earth's atmosphere: Theoretical models. *Icarus* 116:131–153.

Tagliaferri E., Spalding R., Jacobs C., Worden S. P., and Erlich A. 1994. Detection of meteoroid impacts by optical sensors in Earth orbit. In *Hazards due to comets and asteroids*, edited by Gehrels T., Matthews M. S., and Schumann A. Tucson, Arizona: The University of Arizona Press. 199 p.

Tagliaferri E., Spalding R., Jacobs C., and Ceplecha Z. 1995. Analysis of the Marshall Islands fireball of February 1, 1994. *Earth, Moon, and Planets* 68:563–572.

Toth J., Svoren J., Spurný P., Borovička J., Anta I., and Veres P. 2010. The fall of Košice meteorite. Poster presented at Meteoroids 2010 Conference, May 24–28, 2010, Breckenridge, Colorado, USA. http://www.daa.fmph.uniba.sk/meteoritEN.html (08.09.2011).

Trigo-Rodríguez J. M., Borovička J., Spurný P., Ortiz J. L., Docobo J. A., Castro-Tirado A. J., and Llorca J. 2006. The Villalbeto de la Peña meteorite fall: II. Determination of the atmospheric trajectory and orbit. *Meteoritics & Planetary Science* 41:505–517.

Tsvetkov V. I. and Skripnik A. Y. 1991. Atmospheric fragmentation of meteorites according to strength theory. *Astronomicheskii Vestnik* 25:364–371. In Russian.

Weibull W. A. 1951. A statistical distribution function of wide applicability. *Journal of Applied Mechanics* 10:140–147.

Welten K. C., Meier M. M., Caffee M. W., Nishiizumi K., Wieler R., Jenniskens P., and Shaddad M. H. 2010. High porosity and cosmic ray exposure age of asteroid 2008 TC3 derived from cosmogenic nuclides (abstract #2256). 41st Lunar and Planetary Science Conference. CD-ROM.

Yamaguchi U. 1970. The number of test-pieces required to determine the strength of rock. *International Journal of Rock Mechanics and Mining Science* 7:209–227.

Yoshinaka R., Osada M., Park H., Sasaki T., and Sasaki K. 2008. Practical determination of mechanical design parameters of intact rock considering scale effect. *Engineering Geology* 96:173–186.

Zolensky M. E., Nakamura K., Gounelle M., Mikouchi T., Kasama T., Tachikawa O., and Tonui E. 2002. Mineralogy of Tagish Lake: An ungrouped type 2 carbonaceous chondrite. *Meteoritics & Planetary Science* 37:737–761.